

CONDENSATION PHENOMENA IN SUPERSONIC FLOWS

Thesis by  
Joseph V. Charyk

In Partial Fulfillment of the Requirements for the  
Degree of Doctor of Philosophy

California Institute of Technology  
Pasadena, California

August 1946

## TABLE OF CONTENTS

	<u>Page</u>
List of Figures	
Acknowledgment	
Introduction and Summary	i
I. Historical Review of the Phenomenon of Condensation Shock	1
II. Supersaturated Systems	3
III. Critical Supersaturation Conditions	20
IV. Normal Condensation Shock	25
V. Possibility of Continuous Condensation in a Stream of High Water Content	38
VI. Procedure of Computations	42
VII. Illustrative Example	45
VIII. Oblique Shock Waves	48
IX. Applications	50
References	53

## LIST OF FIGURES

- Fig. 1 Variation of Surface Tension With Temperature.
- Fig. 2 Relationship between Temperature and Maximum Supersaturation For Mixture of Air and Water Vapor.
- Fig. 3 Variation of Saturation Vapor Pressure With Absolute Temperature.
- Fig. 4 Comparison of Theoretical and Experimental Critical Supersaturation Curves.
- Fig. 5 Specific Humidity as a Function of Stagnation Pressure for Various Values of the Dew Point.
- Fig. 6a Relationship Between Specific Humidity and Vapor Pressures for Various Values of Total Pressure in Millimeters of Mercury.
- Fig. 6b Relationship Between Specific Humidity and Vapor Pressure for Various Values of Total Pressure in p.s.i.
- Fig. 7 Relationship Between Specific Humidity and Ratio of Mach Numbers After and Before Condensation Shock for Various Initial Mach Numbers  $0 < \sigma < 0.10$ .  $T_1 = 250^\circ\text{K}$ .
- Fig. 8 Relationship Between Specific Humidity and Ratio of Mach Numbers After and Before Condensation Shock for Various Initial Mach Numbers  $0 < \sigma < 0.10$ .  $T_1 = 270^\circ\text{K}$ .
- Fig. 9 Relationship Between Specific Humidity and Ratio of Mach Numbers After and Before Condensation Shock for Various Initial Mach Numbers  $0 < \sigma < 0.10$ .  $T_1 = 300^\circ\text{K}$ .
- Fig. 10 Relationship Between Specific Humidity and Ratio of Mach Numbers After and Before Condensation Shock for Various Initial Mach Numbers  $0 < \sigma < 0.10$ .  $T_1 = 320^\circ\text{K}$ .
- Fig. 11 Relationship Between Specific Humidity and Ratio of Mach Numbers After and Before Condensation Shock for Various Initial Mach Numbers  $0 < \sigma < 0.10$ .  $T_1 = 350^\circ\text{K}$ .
- Fig. 12 Relationship Between Ratio of Mach Number After and Before Shock and Absolute Temperature for Various Values of Initial Mach Number. (Specific Humidity,  $\sigma = 0.005$ )
- Fig. 13 Relationship Between Ratio of Mach Number After and Before Shock and Absolute Temperature for Various Values of Initial Mach Number. (Specific Humidity,  $\sigma = 0.01$ )

- Fig. 14 Relationship Between Ratio of Mach Number After and Before Shock and Absolute Temperature for Various Values of Initial Mach Number. (Specific Humidity,  $\sigma = 0.02$ ).
- Fig. 15 Relationship Between Ratio of Mach Number After and Before Shock and Absolute Temperature for Various Values of Initial Mach Number. (Specific Humidity,  $\sigma = 0.04$ ).
- Fig. 16 Relationship Between Ratio of Mach Number After and Before Shock and Absolute Temperature for Various Values of Initial Mach Number. (Specific Humidity,  $\sigma = 0.06$ ).
- Fig. 17 Relationship Between Ratio of Mach Number After and Before Shock and Absolute Temperature for Various Values of Initial Mach Number. (Specific Humidity,  $\sigma = 0.06$ ).
- Fig. 18 Relationship Between Specific Humidity and Ratio of Mach Numbers After and Before Condensation Shock for Various Initial Mach Numbers.  $T_1 = 250^\circ\text{K}$ .
- Fig. 19 Relationship Between Specific Humidity and Ratio of Mach Numbers After and Before Condensation Shock for Various Initial Mach Numbers.  $T_1 = 270^\circ\text{K}$ .
- Fig. 20 Relationship Between Specific Humidity and Ratio of Mach Numbers After and Before Condensation Shock for Various Initial Mach Numbers.  $T_1 = 300^\circ\text{K}$ .
- Fig. 21 Relationship Between Specific Humidity and Ratio of Mach Numbers After and Before Condensation Shock for Various Initial Mach Numbers.  $T_1 = 320^\circ\text{K}$ .
- Fig. 22 Relationship Between Specific Humidity and Ratio of Mach Numbers After and Before Condensation Shock for Various Initial Mach Numbers.  $T_1 = 350^\circ\text{K}$ .
- Fig. 23 Relationship Between Ratio of Pressures and Ratio of Mach Numbers After and Before Shock for Various Initial Mach Numbers.
- Fig. 24 Relationship Between Ratio of Temperatures and Ratio of Mach Numbers After and Before Shock for Various Initial Mach Numbers.
- Fig. 25 Relation Between Temperature, Pressure, Mach Number and Area Ratio for Sections Downstream of Throat.
- Fig. 26 Determination of Conditions for Collapse of Supersaturated State in Illustrative Example.
- Fig. 27 Relationship Between Supersaturation Pressure Ratio and  $\alpha_x$ .



- Fig. 28 Notation in Treatment of Oblique Condensation Shock.
- Fig. 29 Change in Direction of Flow Through Oblique Condensation Shock.  $M_1 = 1.3$
- Fig. 30 Change in Direction of Flow Through Oblique Condensation Shock.  $M_1 = 2.0$ .
- Fig. 31 Change in Direction of Flow Through Oblique Condensation Shock.  $M_1 = 2.5$ .
- Fig. 32 Change in Direction of Flow Through Oblique Condensation Shock.  $M_1 = 3.0$ .
- Fig. 33 Change in Direction of Flow Through Oblique Condensation Shock.  $M_1 = 4.0$ .

## ACKNOWLEDGMENT

The author is humbly appreciative of the inspiration and encouragement which he has been privileged to receive from Dr. Theodore von Kármán throughout the extent of his graduate study and research.

He would like to thank Dr. Hans-Wolfgang Liepmann for many stimulating discussions, Dr. Homer J. Stewart for his advice and assistance, and Dr. Clark B. Millikan for his interest and guidance.

To Dr. Hsue-shen Tsien, however, the author is indebted not only for his countless valuable suggestions, his wise counsel and the unstinting sacrifice of his time and effort, but infinitely more, for his constant endeavors to instill in the author the zeal and spirit of research that is characteristic of Dr. Tsien. For all this the author is deeply and humbly grateful.

Finally, the author would like to express his indebtedness to the Air Materiel Command of the U.S.A.A.F. under whose sponsorship a major portion of the research program was carried out.

## INTRODUCTION AND SUMMARY

With the very rapid development of jet propulsion systems, the attainment of speeds which seemed to be well beyond reach a few years ago now appears to be at hand. The war has produced many examples of guided missiles travelling at supersonic speeds such as the famed German A-4 rocket, more commonly referred to in this country as the V-2. Today a supersonic airplane is no longer a designer's dream but practically an accomplished fact. Despite the impressive array of symbols of apparent mastery of high speed flight, there exists a large gap of fundamental knowledge that the theoretician working with the experimentalist must fill before true mastery of transonic and supersonic speeds can be said to be at hand. It was only due to the efforts of pioneers in high speed fluid mechanics like de Laval, Riemann, Hugoniot, Lord Rayleigh and Tschaplygin (see for example Ref. 1 to 4) and later the applications of such basic knowledge to the new field of high speed aerodynamics by men with foresight such as Prandtl, Ackeret, von Kármán, Taylor and Busemann (see for example Ref. 5 to 9) that tools for the engineer and designer were available when the need for them suddenly arose.

Today the emphasis of the aeronautical profession is on the basic problems of transonic and supersonic flows. One of the important and at first mystifying phenomena that emerged from experimental investigations in supersonic wind tunnels was the condensation shock. Later such shocks were noticed in the flow over an airfoil in experiments conducted at the California Institute of Technology by Kate Liepmann in 1941. In more recent years their appearance has been noted in

actual flight at high speeds. The importance of such shocks in connection with the aerodynamic characteristics of airfoils in supercritical transonic flow has been pointed out by Tsien and Fejér (Ref. 10). Apparently, however, no detailed investigation of the phenomenon has been made with a view to studying the fundamental aspects of the condensation shock in order to develop practical methods for predicting the occurrence, location, strength and effect of such shocks. It has been the basic purpose of this research to study the detailed aspects of this problem and to endeavor to develop a means of accomplishing the aims noted. It is felt that though crude in many respects, the results of this investigation can provide practical knowledge of basic importance in understanding and treating the problems of condensation shocks when they appear and can point the way towards more refined and detailed future analyses of this problem.

In attacking this problem, an examination of the phenomenon of the sudden collapse of the supersaturated state of the moist air is first made. The assumptions necessary for the determination of the critical stability limit of the supersaturated air are analysed and the necessity for further investigation, especially from the kinetic point of view, is pointed out. The study reveals that the temperature of air at which this collapse occurs is approximately a function only of the amount of water contained in the air and does not depend upon the pressure. This enables an important simplification in the analysis to be made.

The condition for collapse of the supersaturated state is then applied to the special case of normal condensation shocks. Because

of this relatively small amount of water present in air, the effect of the presence of the water on the properties of the air can be neglected except at the shock where the release of the latent heat of vaporization upon condensation is of vital importance. A simple consideration of this heating process yields the interesting result that the flow after the shock must always be supersonic. An important simplification in treating the general condensation problem is an approximation to the actual saturation vapor pressure versus temperature curve by means of an exponential curve. Mathematically this means an approximate integration of the Clausius-Clapeyron equation in the sense that the specific volume of the fluid phase is neglected as compared to the specific volume of the vapor phase. This simplification enables a closed form solution to be obtained.

The oblique condensation shock is then analysed and its application to the flow over an airfoil or other body in a stream of moist air is treated.

The possibility of a continuous condensation instead of an abrupt condensation or a combination of the two is discussed for the case of a one-dimensional flow. Certain interesting results emerge from such a consideration and experimentation will be required to determine whether under certain conditions such a condensation process can take place.

A considerable number of charts are provided which may be of use in making calculations in practical cases. In instances where a different range of values is necessary, additional charts can readily be constructed.

## I. HISTORICAL REVIEW OF THE PHENOMENON OF CONDENSATION SHOCK

Supersaturation phenomena in air and water vapor mixtures have been studied by many investigators for a considerable length of time. Up to quite recently, however, the subject has not been of immediate concern to the aeronautical engineer. In fact, the subject was rather remote from his line of thought so that the first appearance of effects of supersaturation were somewhat mysterious and inexplicable. With the advent of the supersonic wind tunnel, trouble was encountered in producing good flow conditions because of the appearance under certain conditions of a crossing system of compression shocks downstream of the throat. Such shocks were found to vary in location, appearance and strength from day to day and so could not be the result of imperfections in the contours of the walls as at first thought. The phenomenon was discussed by Prandtl (Ref. 11) at the Volta High Speed Conference but no satisfactory explanation for it was advanced at the time. Wieselsberger had also noted such shocks in his high speed wind tunnel experiments and because of their characteristic appearance he had termed them "X-shocks". He suspected correctly that their appearance was associated with the humidity of the air and the experiments of Hermann (Ref. 12) at the Technische Hochschule in Aachen in collaboration with Wieselsberger verified this suspicion and indicated that the so-called "X-shocks" were the result of a sudden condensation of the water vapor originally in the air stream.

A thorough investigation of the mechanism of this condensation phenomenon has been made by Oswatitsch (Ref. 13). He has considered the process of nucleus formation, droplet growth and ultimate collapse

in a detailed manner and has compared the results of his step-by-step calculations with experiments, with resulting excellent agreement.

There is, however, as has been previously stated, an apparent need for a study of the problem with a view to developing a method for predicting the appearance, location, strength and effects of such condensation shocks for practical application purposes. The purpose of Oswatitch's treatment of the problem has, of course, been to inquire into the details of the shock mechanism. For engineering usage, however, such information is usually not required and a treatment of the problem in order to obtain in a simple, direct manner the basic overall information without recourse to a tedious step-by-step calculation is desirable. The present investigation endeavors to do this by making use of several simplifying assumptions and by treating the condensation shock in much the same manner as the ordinary normal shock. In this manner a closed form solution can be obtained which is easily amenable to practical computations.

Such a one-dimensional treatment has certain limitations, however, and it is important to point these out.

For satisfactory high speed wind tunnel operation, condensation shocks are perhaps principally of academic interest, since dehumidifying equipment can be installed to completely eliminate such effects. However, under certain conditions, the problem can be an important one in actual high speed flight since the appearance of a condensation shock can affect in a major fashion the characteristic properties of an airfoil section. It is, therefore, of considerable interest to obtain an understanding of the physical process itself and to develop tools for efficient practical application.

## II. SUPERSATURATED SYSTEMS

Air is said to be saturated when the contained vapor is in equilibrium with a plane surface of pure water at the same temperature. This means that as many molecules pass from the liquid to the vapor phase per unit time as pass from the vapor to the liquid phase. It is possible, however, under certain conditions for the air to become supersaturated, that is, to contain more water vapor than is sufficient for saturation at that temperature.

R. von Helmholtz in 1887 had drawn attention to supersaturation under certain conditions. He observed that a saturated steam jet issuing from an orifice of about 0.08 inches diameter into the open remained as clear as the air close to the orifice and that only after some distance from the origin did it begin to cloud. Another important observation of Helmholtz was that an electrical discharge between two pointed terminals so arranged as to penetrate the jet made the jet appear still more cloudy. This was important from the standpoint that it illustrated that ions were of assistance in causing condensation to occur, that is, they are nuclei upon which droplets can collect.

The Wilson "cloud" chamber provided another interesting example of supersaturated conditions. It was found in initial experiments that if the saturated air contained a large number of dust particles, intense cloudiness was immediately formed upon expansion. However, if attempts were made to eliminate in so far as possible all the dust particles, an expansion up to 1.38 times the initial volume could be obtained with no visible condensation but that any further expansion



apparently resulted in a collapse of the supersaturated state with the resultant formation of a heavy cloud. Here again, ions were found to have the same effect as dust particles, that is, to assist in condensation. This effect led to very important applications of the Wilson cloud chamber in experimental nuclear physics. It enabled the paths of charged particles to be observed visually by means of the tracks formed by the condensation of small water particles along the route taken by the particle. It is safe to ascert that the cloud chamber has proved to be one of the most valuable tools in nuclear physics research.

Experimental investigations into determining the amount of supersaturation possible, the effect of nuclei such as ions and dust particles and other phases of the problem have been extensively carried on. Wilson concluded that other types of nuclei must be always present in an inexhaustible supply and appeared to form an essential part of the water vapor since they could not be removed by any process. Hirn and Cazin (Ref. 14), Yellott (Ref. 15), Stodola (Ref. 16), Binnie (Ref. 17), and others used different experimental techniques in studying this problem. One of the particular engineering applications demanding some of these later researches was the steam turbine. It seemed somewhat surprising, therefore, in view of this wealth of background, that the phenomenon was unrecognized when it first stepped into the direct domain of the aeronautical engineer in the supersonic wind tunnel.

In analysing the amount of supersaturation possible before collapse occurs, one of the fundamental problems is to ascertain the type of

mechanism involved in nucleus formation in the absence of dust particles or ions. To do this it is necessary to first investigate the equilibrium conditions for water droplets in a stream of moist air.

The saturation vapor pressure,  $p_{\infty}$ , is the maximum pressure which water vapor can exert when in contact with a plane surface of pure water. If a curved surface is considered, as in the case of droplets, the equilibrium pressure,  $p_v$ , is greater than the saturation vapor pressure by reason of the "capillary" forces. The relationship between this pressure ratio and the other fundamental parameters involved was first established by W. Thomson, (later Lord Kelvin, Ref. 18).

This relationship is of fundamental importance in understanding the phenomenon of supersaturation which is directly responsible for condensation shocks. It may be of value, therefore, to discuss in some detail the derivation of the Thomson formula.

Consider a curved surface formed by holding in a liquid a capillary tube of a material such that the liquid does not wet it and let  $h$  represent the depression of the liquid in the capillary tube. The curved surface is approximately a part of a sphere if the diameter of the tube is sufficiently small. The liquid is assumed to be in a closed vessel with the space above the free surface being occupied by the vapor of the liquid. The system is assumed to be in equilibrium at a temperature  $T$ .

The difference between the pressures  $p_v$  and  $p_{\infty}$  clearly must be equal to the weight of the vapor column in the tube. Let  $\rho_v$  be the density of the vapor. If the vapor is assumed to obey the perfect gas law:

$$p_v = \frac{\rho_v m_v}{RT} \quad (1)$$

where

$m_v$  = molecular weight of vapor

$p$  = vapor pressure

$R$  = universal gas constant

Just under the curved surface the pressure  $p'_\infty$  is clearly given by the relation:

$$p'_\infty = p_\infty + \rho h \quad (2)$$

where

$\rho$  = density of liquid

The difference between  $p_v$  and  $p'_\infty$  arises from the surface tension forces. If  $S$  is the surface tension of the liquid and  $r$  the radius of the tube, equilibrium considerations yield the following relation

$$\pi r^2 (p'_\infty - p_v) = 2\pi r S \quad (3)$$

$$\text{or} \quad p'_\infty - p_v = \frac{2S}{r} \quad (4)$$

From equation (2),

$$p_\infty + \rho h - p_v = \frac{2S}{r} \quad (5)$$

Since the difference between  $p_v$  and  $p_\infty$  arises solely from the weight of the vapor column

$$p_v - p_\infty = \int p_v dh = \rho h - \frac{2S}{r} \quad (6)$$

$$\text{or} \quad \frac{2S}{r} = \int (p - p_v) dh \quad (7)$$

Now,

$$p_v dh = dp \quad (8)$$

Combining equations (1), (7) and (8) the following relation is obtained:

$$\frac{2S}{r} = \int_{p_\infty}^{p_v} \frac{(p - p_v)}{p_v} dp \cong \frac{RTp}{m_v} \int_{p_\infty}^{p_v} \frac{dp}{p} \quad (9)$$

or

$$\ln \frac{p_v}{p_\infty} = \frac{2S}{r} \cdot \frac{m_v}{R_p T} \quad (10)$$

This is the Thomson formula and expresses the relation of the pressure  $p_v$  in the supersaturated vapor around a spherical drop of radius  $r$  to the normal saturation pressure,  $p_\infty$ . This formula will, of course, lose its validity as  $r$  approaches zero since in such a case molecular processes will become of major importance and the assumptions under which the formula was derived will be violated.

The vapor pressure,  $p_v$ , is only stable under certain conditions, namely when the fluid phase is not present. The terminology "metastability" has been used by Ostwald to denote this kind of stability. The reason for this metastability is associated with the work which must be done against capillary forces in the establishment of a new phase. If such forces are neglected it is possible to show on the basis of classical theory that a supersaturated state cannot exist for any finite length of time. It seems reasonable, therefore, to take as a measure of the metastability of a supersaturated system, the work which must be done against the capillary forces in order to produce a state in which further formation of the new phase occurs voluntarily. If a droplet of the characteristic radius,  $r$ , as given by the Thomson formula has been produced it requires only an infinitesimal amount of work to produce an instability. The work necessary for the production of such a droplet can be readily calculated. First, however, it may be of value to discuss in a general manner how droplets of this characteristic size can be formed. In a mixture of air and water vapor, collisions continually occur between the water vapor molecules

with the resultant formation of minute droplets of the fluid phase. These droplets will, of course, revert to the vapor phase almost immediately since the vapor is undersaturated with respect to them. However, on a statistical basis, a sufficiently large number of molecules will occasionally be involved in a single collision such that a water droplet of the characteristic size is formed. Such a droplet will now no longer decompose but will grow by the addition of other vapor molecules. The term "condensation nuclei" or "condensation germs" is usually attached to such droplets. The condensation shock, therefore, is nothing more than the very rapid formation of many such condensation nuclei which brings about the collapse of the supersaturated state.

Since the latent heat of vaporization is released upon condensation, one of the essential elements in the growth of a droplet is that the necessary heat transfer away from the surface of the droplet must be provided for. If this heat were not removed rapidly, the resulting temperature rise would cause a saturation limit to be reached and further droplet growth would cease. In addition to the heat transfer away from the droplet, there must be provision for the associated transfer of mass required for the droplet growth. The relative importance of heat conduction and diffusion processes in providing for the necessary mass and heat transfer is not too clear at present. Investigators in the field of chemical kinetics have begun studies into related problems particularly as concerns combustion processes and the results of their work should be of considerable value in obtaining an understanding of this complex problem.

A systematic study of the problem of the production of condensation nuclei was first made by Volmer and Weber (Ref. 19). Let  $p_v$  denote the pressure outside of a droplet and  $p_v'$  the pressure existing within a droplet of radius  $r$ . If  $S$  is the surface tension, the following relation follows directly from equilibrium considerations:

$$(p_v' - p_v) \pi r^2 = 2 \pi r S \quad (11)$$

or

$$p_v' - p_v = \frac{2S}{r} \quad (12)$$

Now during the formation of such a droplet, the volume of the droplet is increased from zero to  $\frac{4}{3} \pi r^3$ . Since the pressure  $p_v'$  inside of the droplet is larger than the pressure  $p_v$  outside of the droplet, this increase in volume of the droplet corresponds to a work release  $W_1$  equal to the product of  $(p_v' - p_v)$  and  $\frac{4}{3} \pi r^3$ . Thus according to (12)

$$W_1 = \frac{2S}{r} \cdot \frac{4}{3} \pi r^3 = \frac{2}{3} \cdot 4 \pi r^2 S \quad (13)$$

However, simultaneously the surface area of the droplet increases from 0 to  $4 \pi r^2$ . The work  $W_2$  done against the surface tension is thus

$$W_2 = 4 \pi r^2 S \quad (14)$$

The difference  $W$  of  $W_2$  and  $W_1$  is thus the network required to form such a droplet. Therefore,

$$W = W_2 - W_1 = \frac{1}{3} \cdot 4 \pi r^2 S = \frac{1}{3} F S \quad (15)$$

where  $F$  is the surface area of a droplet of radius  $r$ , or  $4 \pi r^2$ .

If the droplet is of the critical dimension given by the Thomson formula (10),  $r$  can be eliminated from Equation (15) by introducing the vapor pressures. Thus

$$W = \frac{16 \pi S^3 m_v^2}{3 R^2 T^2 p^2 \left[ \ln \frac{p_v}{p_{\infty}} \right]^2} \quad (16)$$

For a plane surface, i.e.,  $p_v = p_\infty$  it is clear from the above equation that  $W = \infty$ . This means that vapor of pressure  $p_\infty$  is absolutely stable. As  $p_v$  increases the stability correspondingly decreases.

The frequency  $J$  of the formation of droplets of the critical size can be shown by considerations based on statistical thermodynamics to be proportional to  $e^{-\frac{W}{RT}}$  where  $T$  is the temperature at which the process takes place and  $W$  denotes the work required for the formation of such a droplet.

Therefore:

$$J = K e^{-\frac{W}{RT}} \quad (17)$$

$$= K e^{-\frac{SF}{3RT}} \quad (18)$$

By use of formula (16) the frequency  $J$  can also be expressed in the form:

$$J = K e^{-\left[ \frac{16 \pi S^3 m_v^2}{3 R^3 T^3 \rho^2} \left( \ln \frac{p_v}{p_\infty} \right)^2 \right]} \quad (19)$$

The factor  $K$  in this expression is not determined as a result of the thermodynamic considerations outlined above. Kinetic considerations can be utilized, however, to obtain an expression for the nucleus formation frequency  $J$ . In other words, thermodynamic considerations alone cannot determine the constant of proportionality  $K$ . Various methods of attack on this problem have been used by various authors, and there is some disagreement as to the validity of certain approaches. Such kinetic considerations have been made by Volmer and Weber (Ref. 19), Farkas (Ref. 20), Stranski and Kaischew (Ref. 21) and Becker and Doring (Ref. 22). The latter authors have arrived at essentially the same result as Farkas by a somewhat more satisfying argument and the

results of their considerations are used herein. Becker and Döring have objected to the results of Kaischew and Stranski on the basis that the equations of the kinetic theory which refer to the vaporization and condensation of individual molecules are used in a differential equation whereas they are defined only for integer values of  $n$  where  $n$  is the number of molecules. Also integration then yields new constants whose determination cannot be made in a satisfactory manner.

Becker and Döring, on the other hand, have used simply a set of algebraic equations and by a pure algebraic elimination process have obtained the desired result directly. A great deal of work has also been done by the authors listed above towards the solution of the problem where conditions are such that ice crystals are formed rather than droplets. The mechanism of crystal formation is not very well understood at the present time and considerable experimentation must yet be pursued before the theoretical results obtained could be applied with complete confidence. For this reason this case will not be treated in the present investigation but the assumption will be made that water droplets first form to produce the condensation shock. Subsequent formation of ice, therefore, would not affect the results derived.

In the determination of the constant  $K$ , the method of Becker and Döring will be used. This is characterized by an interesting analogy which permits of a ready solution for  $K$  in a simple clear manner. The method is particularly adaptable with some modification to the case of ice crystal formation.



Becker and Döring consider a quasi-stationary condensation process in which the vapor pressure in a large vessel is maintained constant by the addition of individual molecules. Droplets continually form and begin to grow. It is supposed that as soon as a droplet has grown to a certain extent it is removed from the vessel. The amount of growth is specified by stating that the droplet is removed when it contains  $s$  molecules, which number is greater than the number of molecules,  $n$ , in a droplet of the critical size.

At any instant, therefore, there will be droplets of various sizes within the vessel. Suppose that  $N_\nu$  is the number of droplets which contain exactly  $\nu$  molecules. In this notation, therefore,  $N_1$  is the number of free vapor molecules while  $N_s = 0$ . The surface area of a droplet which contains  $\nu$  molecules is taken to be  $F_\nu$ . Consider  $a_0$  to be the probability that one molecule condenses on a unit surface area and  $q_\nu$  to be the probability that one molecule leaves a unit surface area of a droplet composed of  $\nu$  molecules per unit of time. The total surface area of all droplets composed of  $\nu$  molecules is  $N_\nu F_\nu$ .

Let this total be denoted by  $N'_\nu$ . Then the nucleus formation frequency  $J$  can be expressed by the relation

$$J = a_0 N'_{\nu-1} - q_\nu N'_\nu \quad \text{for all } \nu \quad (20)$$

$$\text{Let } \beta_\nu = a_0 / q_\nu \quad (21)$$

$$\text{Then } N'_\nu = \beta_\nu N'_{\nu-1} - J \beta_\nu / a_0 \quad (22)$$

The quantity  $\beta_\nu$  increases monotonically with increasing  $\nu$  and is evidently equal to unity when  $\nu = n$ , the number of molecules for forming a droplet of critical size.

To determine  $\beta$ , one must, strictly speaking, investigate the problem from the point of view of kinetic theory. In other words, one must consider the collisions between the molecules in the droplet, the collisions between the molecules in the droplet and the molecules in the vapor, and the collisions between the molecules in the vapor. When these collision processes are determined, one can then calculate the ratio  $\beta$ , for the average rate of molecules joining the droplet and the average rate of molecules leaving the droplet. However, such a detailed analysis is hardly practical at present due to the rather scanty knowledge of the liquid state. To avoid this difficulty, one has to adopt a method of considering the droplet at a state of quasi-equilibrium and to arrive at an approximate evaluation of the quantity  $\beta$ . In such a calculation, one assumes that the average ratio  $a_0$  at which the molecules join the droplet is the same as the average rate at equilibrium conditions. This assumption would be a good approximation if the growth of the droplet is slow in the time-scale for molecular collisions. Since under ordinary conditions, the time scale for molecular collisions is of the order of  $10^{-10}$  seconds, which is much shorter than the time intervals required for the collapse of the supersaturated state, the quasi-equilibrium hypothesis is a satisfactory one.

With this assumption, and denoting the molecular mass by  $m$  and mean molecular velocity by  $v$ , the pressure  $p_v$  in the Thomson formula (10) must be proportional to  $a_0 \cdot mv$ .

Thus

$$a_0 = \frac{p_\infty}{m v} e^{-\frac{2Sm_v}{RT\beta} \cdot \frac{1}{r_m}} \quad (23)$$

Since for  $\nu = n$ ,  $a_0 = q_n$ , therefore

$$q_n = \frac{p_\infty}{m\nu} e^{\frac{2Sm\nu}{RT\rho} \cdot \frac{1}{r_n}} \quad (24)$$

For other values of the radius  $r_\nu$ , corresponding to the number  $\nu$  of molecules in the droplet, one uses the same dependence of  $q$  on  $r$ , i.e.,

$$q_\nu = \frac{p_\infty}{m\nu} e^{\frac{2Sm\nu}{RT\rho} \cdot \frac{1}{r_\nu}} \quad (25)$$

Then the ratio  $\beta_\nu$  is

$$\beta_\nu = \frac{a_0}{q_\nu} = e^{\frac{2Sm\nu}{RT\rho} \left[ \frac{1}{r_n} - \frac{1}{r_\nu} \right]} \quad (26)$$

With the ratio  $\beta_\nu$  so determined one can proceed with the calculation. Equation (22) gives the following set of relations

$$\begin{aligned} N_{\nu+1}' &= N_\nu' \beta_{\nu+1} - J/a_0 \beta_{\nu+1} \\ N_{\nu+2}' &= N_{\nu+1}' \beta_{\nu+2} - J/a_0 \beta_{\nu+2} \\ &\dots\dots\dots \\ &\dots\dots\dots \\ N_s' &= N_{s-1}' \beta_s - J/a_0 \beta_s \end{aligned} \quad (27)$$

Equation (27) can be expressed in the general form:

$$\phi_{i+1} = \phi_i - JR_i \quad (28)$$

where

$$\phi_i = \frac{N_i'}{\beta_2 \beta_3 \dots \beta_i} \quad \text{and} \quad R_i = \frac{1}{a_0 \beta_2 \beta_3 \dots \beta_i}$$

Equation (28) can be considered from a very simple viewpoint if  $J$  is considered as an electric current flowing from the point  $i$  to the

point  $i + 1$  with  $(\phi_i - \phi_{i+1})$  as the potential difference and  $R_i$  as the resistance.

From equation (28) we have in particular:

$$\phi_s - \phi_s = J [R_s + R_{s+1} + \dots + R_{s+1}] \quad (29)$$

It can be noted that:

$$\phi_1 = N_1', \quad \phi_s = 0$$

For the critical number of molecules,  $n$ , the quantity  $\beta_n = 1$ .

It can be noted that for  $\nu < n$  the quantity  $\beta_\nu$  will be less than one and for  $\nu > n$ , the quantity  $\beta_\nu$  will be greater than one. It is clear therefore, that the resistance  $R_i$  will have a maximum at  $i = n$ .

$$R_i = \frac{1}{a_0} e^{\frac{2Sm_\nu}{RT\rho} \left[ \frac{1}{r_2} + \frac{1}{r_3} + \dots + \frac{1}{r_i} - \frac{i-1}{r_n} \right]} \quad (30)$$

It is convenient to introduce a new variable,  $x_\nu$ , defined as the ratio between the radius of a droplet consisting of  $\nu$  molecules and one consisting of  $n$  molecules.

$$x_\nu = r_\nu / r_n \quad (31)$$

Now the number of molecules,  $n$ , in a droplet of radius  $r_n$  is given by:

$$n = \frac{4}{3} \pi r_n^3 \cdot \frac{\rho}{m_\nu} \quad (32)$$

Therefore,

$$x_\nu = \left( \frac{\nu}{n} \right)^{1/3} \quad (33)$$

or,

$$\begin{aligned} \nu &= n x_\nu^3 \\ d\nu &= 3n x_\nu^2 dx \end{aligned}$$

The exponent in the equation for the resistance,  $R_i$ , can now be written as:

$$\begin{aligned} \frac{1}{\lambda_2} + \frac{1}{\lambda_3} + \dots + \frac{1}{\lambda_i} &\cong \frac{1}{\lambda_n} \int_{y=1}^{y=i} \frac{dy}{x_y} \\ &= \frac{3m}{\lambda_n} \int_{x_1}^{x_i} x dx \\ &= \frac{3m}{2\lambda_n} (x_i^2 - x_1^2) \end{aligned} \quad (34)$$

Also

$$i-1 = n(x_i^3 - x_1^3) \quad (35)$$

Therefore

$$R_i = \frac{1}{a_0} e^{\frac{Sn}{\lambda_n} \cdot \frac{m_v}{RT\rho} [3x_i^2 - 3x_1^2 - 2x_i^3 + 2x_1^3]} \quad (36)$$

From equation (15) and (32), this can be written in the form:

$$R_i = \frac{1}{a_0} e^{\frac{SF}{3RT} [(3x_i^2 - 2x_i^3) - (3x_1^2 - 2x_1^3)]} \quad (37)$$

where  $F$  = surface area of a droplet of the critical size.

The summation over all the individual resistances can be replaced by an integration as follows:

$$\begin{aligned} \int_1^s R_y dy &= 3m \int_{x_1}^{x_s} R(x) \cdot x^2 dx \\ &= \frac{3m}{a_0} e^{-\frac{SF}{3RT} (3x_1^2 - 2x_1^3)} \int_{x_1}^{x_s} e^{\frac{SF}{3RT} (3x^2 - 2x^3)} x^2 dx \end{aligned} \quad (38)$$

Since in an actual case the quantity  $\frac{SF}{3RT}$  is rather large, the integrand possesses a strong maximum at  $x = 1$ . Because of this feature an accurate approximation to the actual value of the integral can readily be made.

Let  $x = 1 + \xi$  (39)

Then:

$$\int_{x_1}^{x_2} e^{\frac{SF}{3RT} (3x^2 - 2x^3)} x^2 dx = e^{\frac{SF}{3RT}} \int_{x_1-1}^{x_2-1} e^{-\frac{SF}{3RT} (3\xi^2 + 2\xi^3)} (1+\xi)^2 d\xi \quad (40)$$

Because of the numerical value of the quantity  $\frac{SF}{3RT}$  in the exponent, the above term can be approximated without a considerable error by:

$$e^{\frac{SF}{3RT}} \int_{-\infty}^{\infty} e^{-\frac{SF}{3RT} \cdot 3\xi^2} d\xi \quad (41)$$

The total resistance:

$$R = \frac{3n}{a_0} e^{\frac{SF}{3RT} (1 - 3x_1^2 + 2x_1^3)} \int_{-\infty}^{\infty} e^{-\frac{SF}{3RT} \cdot 3\xi^2} d\xi \quad (42)$$

$$= \frac{3n}{a_0} e^{\frac{SF}{3RT} (1 - 3x_1^2 + 2x_1^3)} \frac{\sqrt{\pi}}{\sqrt{\frac{SF}{RT}}} \quad (43)$$

$$\cong \frac{3n}{a_0} e^{\frac{SF}{3RT}} \frac{\sqrt{\pi}}{\sqrt{\frac{SF}{RT}}} \quad (44)$$

If it is noted that  $\phi_1 = N_1'$ , then equations (28) and (44) yield the following expression for the nucleus formation frequency, J:

$$J = \frac{a_o N_1'}{3n} \sqrt{\frac{SF}{\pi RT}} e^{-\frac{SF}{3RT}} \quad (45)$$

If this expression is compared with equation (18), it is seen that:

$$K = \frac{a_o N_1'}{3n} \sqrt{\frac{SF}{\pi RT}} \quad (46)$$

In the above expression  $N_1'$  is the total surface area of free molecules. Then  $a_o N_1'$  is twice the number of gas kinetic collisions which take place between the vapor molecules. The number of such collisions per cubic centimeter is proportional to the number of vapor molecules per cubic centimeter. If  $v$  is the mean molecular velocity,  $l$  the mean free path and  $C$  the number concentration,

$$a_o N_1' = C \frac{v}{l} \quad (47)$$

The mean free path  $l$  is inversely proportional to the concentration,  $C$ , if the effect of the presence of other molecules on the water vapor molecules is neglected. Therefore:

$$a_o N_1' = C^2 \frac{v}{l_o C_o} \quad (48)$$

The subscript  $o$  denotes conditions at standard temperature and pressure, i.e., a temperature of 273°K and a pressure of 760 millimeters of mercury.

By use of the results of kinetic theory, equation (48) can be expressed in a more convenient form:

$$a_o N_1' = L \sqrt{\frac{8}{\pi R}} \frac{T_o}{p_o l_o} \cdot \frac{1}{\sqrt{m_v}} \cdot \frac{p^2}{T^{3/2}} \quad (49)$$

where  $L = \text{Avogadro's number}$   
 $= 6.023 \times 10^{23}$   
 $R = \text{Universal gas constant}$   
 $= 0.831 \times 10^8 \text{ ergs/}^\circ\text{C.}$

From thermodynamic considerations, the general form of the expression for the nucleus formation frequency has been established and kinetic considerations have led to an expression for the constant which was undetermined on the basis of the original considerations.



### III. CRITICAL SUPERSATURATION CONDITIONS

As has been emphasized previously, the important part of the expression for the nucleus formation frequency,  $J$ , is the exponential term. A plot of  $\ln J$  versus  $\ln(p_v/p_\infty)$  for a given temperature in the range considered ( $200 < T < 360^\circ\text{K}$ ) is characterized by a very steep slope so that a minor change in the quantity  $\ln p_v/p_\infty$  results in a tremendous variation in  $J$ , the nucleus formation frequency. This is noteworthy in that from a physical standpoint it means that nuclei begin to form and grow at a very rapid rate. From a practical computation standpoint it is important in that it is found to be of little consequence whether the critical value of  $\ln p_v/p_\infty$  for a given temperature is taken to be the intercept of this curve with the  $\ln p_v/p_\infty$  axis or whether it is taken to be the value of  $\ln p_v/p_\infty$  when  $J$  is 100 or 1000. This rapid increase of the number of condensation nuclei implies a collapse of the supersaturated state or a condensation shock.

Actually the process is, of course, not a sudden one, but rather the nuclei begin to form slowly at first and then more and more rapidly. For purposes of discussion of a condensation shock, it seems reasonable, however, to neglect the effects of the few condensation nuclei and to simplify the considerations by assuming that nothing happens until conditions are such as to cause a very rapid growth of condensation nuclei. It is felt that this assumption introduces only very slight errors which are probably well within the limits of accuracy of other phases of the general problem.

On this basis it is therefore theoretically possible to determine a relationship between temperature and  $\ln p_v/p_\infty$  or the degree of supersaturation possible before a collapse of the supersaturated state

occurs. This relationship will be referred to as the critical supersaturation curve. This curve is of extreme importance in that it provides a theoretical means for predicting the conditions for the occurrence of a condensation shock and together with a knowledge of wind tunnel diffuser shape or airfoil contour together with the free stream conditions enables one to predict the location of such a shock.

The expression for the nucleus formation frequency can now be written:

$$J = \frac{a_0 N_1'}{3n} \sqrt{\frac{SF}{\pi RT}} e^{-\frac{SF}{3RT}} \quad (50)$$

where

$$SF = \frac{16 \pi S^3 m_v^2}{R^2 T^2 \rho^2 [\ln p/p_\infty]^2}$$

In carrying out the calculations for the determination of the critical supersaturation curve, some uncertainty in the proper numerical values for the various quantities in equation (50) was evident. For example, there is reason to suspect that the value for the surface tension  $S$  is affected by the time scale involved in an experiment. There is also doubt as to the correct value at low temperatures. Here, particularly, the effect of dynamic conditions is dominant. For lack of any definite knowledge, dynamic considerations were neglected and the variation of surface tension with temperature was considered to be that shown in Figure 1.

As far as the other parameters in equation (50) are concerned, chief uncertainty is in the appropriate value for the mean free path,  $l_0$ , at S.T.P. This is of comparatively minor importance, however, since this parameter does not appear in the exponent, but in the con-

stant whose exact determination is not essential.

From equation (49)

$$a_0 N_1' = L \sqrt{\frac{8}{\pi R}} \frac{T_0}{p_0 l_0} \cdot \frac{1}{\sqrt{m_v}} \cdot \frac{p^2}{T^{3/2}}$$

If  $p$  is expressed in millimeters or mercury, the following numerical values enter:

$$\begin{aligned} a_0 N_1' &= 6.023 \times 10^{23} \sqrt{\frac{8}{\pi \cdot 0.831 \cdot 10^8}} \cdot \frac{273}{760} \cdot \frac{13.6}{10} \cdot 980 \cdot \frac{p^2}{l_0 \sqrt{m_v} T^{3/2}} \\ &= 5.05 \cdot 10^{22} \frac{p_\infty^2}{l_0 \sqrt{m_v} T^{3/2}} \left( \frac{p}{p_\infty} \right)^2 \end{aligned}$$

where  $l_0$  is taken to be  $10^{-5}$  cm.

From equation (18)

$$\ln J = \ln K - \frac{S F}{3RT}$$

The critical supersaturation curve thus derived is plotted in Figure 2 for a range of temperatures from  $270^\circ\text{K}$  to  $360^\circ\text{K}$ . The saturation vapor pressure versus temperature relation used in these computations was that indicated by the solid curve in Figure 3. For a lower range of temperatures, greater uncertainties arise principally by reason of ignorance as to the appropriate value for the surface tension. Since, as has been previously stated, the dominant term in the expression for the nucleus formation,  $J$ , is the exponential one, ignorance of the correct values of some of the parameters forming the constant  $K$  is of only minor influence. Variations in quantities in the exponential term, as, for example, the surface tension, will have a marked effect on the critical supersaturation curve. It has already been pointed out that there is some reason to believe that the surface tension may be affected by the rate of expansion, or what might be termed the time-scale.

The effect of the presence of dust particles and ions has also been completely neglected in the calculation of the critical supersaturation curve. Unless these are present in extremely large numbers, it seems unlikely that they can seriously influence the condensation conditions. The interval of time between the attainment of saturation conditions and the final collapse of the supersaturated state is so short in all cases under discussion here that even though some condensation begins to occur around the dust particles or ions this condensation cannot reach any appreciable proportions before millions of condensation nuclei form according to the considerations of the present investigation. This produces the sudden collapse of the supersaturated state and the condensation shock. Since the formation of small numbers of nuclei, which begin to form immediately after saturation conditions are attained, is neglected and only the very rapid growth at critical supersaturation is considered, the neglect of the effect of the presence of dust particles or ions is believed to be justified.

Subsequent to the theoretical determination of the critical supersaturation curve as discussed above, it was brought to the author's attention that some experimental work had been done in Germany (Ref. 23) with the aim of obtaining data which could be used for the establishment of maximum critical supersaturation conditions. On the basis of these experiments, the following empirical formula was found to be satisfactory above 210°K if no ions were present:

$$\ln p_r/p_\infty = \frac{780}{T} - 1.521 \quad (51)$$

Ice crystal formation was not observed above this temperature, and below it, the following empirical law was established:

$$\ln p_r/p_\infty = \frac{1373}{T} - 3.748 \quad (52)$$

No attempt was made in the present investigation to take into account conditions when ice crystals formed, but a comparison of formula (51) with the present theoretical critical supersaturation curve is shown in Fig. (4). It is interesting to note that agreement is excellent for the higher values of temperature and that serious discrepancies arise only for the lower temperature range considered where deviations were expected on the basis of the very meager experimental data whose use was necessary in the present theoretical determination of such a curve.

Further experimentation would certainly appear to be desirable for the purpose of determining the relative importance of such factors as the presence of various quantities of artificial nuclei, the effect of dynamic conditions, low temperature behavior, ice crystal formation and so on. The second item above is of particular importance in the present study since the empirical formulae (51 and 52) were obtained with the mixture of water vapor and air initially at rest. The question as to the extent of validity of such data in an application where marked velocity gradients exist, as will be the case for any of the high speed flows under consideration here, remains as yet unanswered. There appears to be a need for considerable experimental research before a satisfactory understanding of critical supersaturation conditions can be obtained for cases where the mixture itself is moving at high speeds.

#### IV. NORMAL CONDENSATION SHOCK

Once the conditions for the occurrence of a condensation shock or the breakdown of the supersaturated state have been established, the next problem is to determine the strength of the shock. In other words, it is desired to know the change in Mach number, change in pressure and change in temperature across the shock. If the usual assumptions of one-dimensional gas dynamics are made it is possible to treat a condensation shock in much the same manner as a normal shock is treated in ordinary one-dimensional gas dynamics (Ref. 24).

By use of the critical supersaturation curve and the common one-dimensional gas flow equations, the position of occurrence of the condensation shock and the temperature, pressure and Mach number before the shock can be determined. The subscript 1 will be used to denote conditions before the shock while the subscript 2 will be used to denote conditions after the condensation shock. The strength of a condensation shock must clearly depend on the amount of water vapor present in the air stream. The most convenient parameter to express this quantity is the specific humidity which will be denoted by  $\sigma$  and which is the mass ratio of water vapor to air plus water vapor. Thus, if  $W_a$  is the mass of dry air flowing by a given point per unit time and  $W_v$  is the mass of water vapor flowing by the same point in the same time interval, then

$$\sigma = \frac{W_v}{W_v + W_a} \quad (53)$$

If  $f$  is the cross-sectional area of the section through which the mixture of dry air and water vapor is flowing and  $u$  is the velocity of the stream,

$$W_v = f u \rho_v \quad (54)$$

where  $\rho_v$  = density of water vapor.

$$W_a = f u \rho_a \quad (55)$$

where  $\rho_a$  = density of air.

Therefore,

$$\sigma = \frac{p_v}{p_v + p_a} \quad (56)$$

It is assumed that the air and the water vapor obey the perfect gas law, i.e.

$$p_a = \frac{\rho_a RT}{m_a}$$

$$p_v = \frac{\rho_v RT}{m_v} \quad (57)$$

where T = Equilibrium temperature of mixture of air and water vapor.

$m_a$  = Molecular weight of dry air.

$m_v$  = Molecular weight of water vapor.

From Dalton's law of partial pressures it is known that in a mixture of several gases the pressure exerted by each gas is the same as that which it would exert if it were the only gas present. Therefore, if p is the total pressure of the water-vapor-air mixture, by the above law:

$$p = p_a + p_v \quad (58)$$

Substituting equations (57) and (58) into (56), the following expression is obtained for the specific humidity:

$$\sigma = \frac{p_v}{p(k+1) - p_v k} \quad \text{where } k = \frac{m_a - m_v}{m_v} \quad (59)$$

If  $p_\infty$  is the saturated vapor pressure, then the relative humidity, r, is defined as the ratio of the vapor pressure to the saturated vapor pressure.

$$r = \frac{p_v}{p_\infty} \quad (60)$$

The relationship between the specific humidity and the relative humidity is then:

$$\sigma = \frac{r}{\frac{p}{p_{\infty}} (k + 1) - r.k.} \quad (61)$$

In general, however, the dew point is a more satisfactory parameter to use than the relative humidity. This is certainly true in this investigation since for the range of parameters used a very simple chart can be constructed for the determination of the specific humidity. If the specific humidity is plotted versus the stagnation pressure for various values of the dew point, the curves on log paper are straight lines at  $45^{\circ}$ . Thus, to determine the specific humidity it is necessary only to measure the stagnation pressure and the dew point. The specific humidity determination chart is shown in Figure 5. By use of standard tables, (Ref. 25) the chart can easily be extended for other values of the dew point.

If the relative humidity were used instead of the dew point, it would be necessary to construct a new chart for every temperature. For this reason the dew point is a much more logical parameter for this case.

Equation (59) can be used to determine the vapor pressure in a mixture of air and water vapor if the total pressure and the specific humidity are known.

$$p_v = p \frac{(k + 1)}{k\sigma + 1} \cdot \sigma \quad (62)$$

Fig. 6(a) or 6(b) provides a graphical means for this determination.

In setting up the general shock equations, it will be necessary to make several assumptions in addition to those made in the treatment



of ordinary normal compression shocks. It will be assumed:

- i) that the mixture of vapor and air after the collapse of the supersaturated state is a saturated one, i.e., the vapor pressure is the saturated vapor pressure corresponding to the temperature after the condensation shock.
- ii) that the only heat addition is that due to the release of the heat of vaporization upon condensation.
- iii) that the necessary heat transfer is provided for so that the heat released is very rapidly distributed in a uniform manner throughout the mixture.
- iv) that the original humidity is small enough so that the total energy of the liquid phase after condensation may be neglected in the energy equation. Since in all practical cases the humidity is small enough, it was not considered necessary to introduce additional complications by the inclusion of these terms. For a better approximation this could be done.
- v) that no condensation occurs until the critical supersaturation conditions as given by Figure 2 are reached and that then the supersaturated state completely collapses. The necessary mass transfer for this is assumed to be provided.
- vi) that the presence of dust particles or other such nuclei in the air stream does not effect the conditions for condensation. Whereas this is a bad assumption for static conditions, its validity under supersonic flow conditions is probably quite good. This point will be discussed to some extent later.

The basic equations may now be formulated as follows:

1) Continuity

$$\rho_1 u_1 = \rho_2 u_2 \quad (63)$$

2) Momentum

$$p_1 + \rho_1 u_1^2 = p_2 + \rho_2 u_2^2 \quad (64)$$

3) Energy

$$\frac{u_1^2}{2} + \frac{a_1^2}{\gamma-1} + L(\sigma_1 - \sigma_2) = \frac{u_2^2}{2} + \frac{a_2^2}{\gamma-1} \quad (65)$$

$\gamma = C_p/C_v$  for mixture  $\approx C_p/C_v$  for air if  $\sigma$  is small, and

$a$  = velocity of sound in mixture

$$\approx \sqrt{\frac{\gamma R T}{m_a}} \quad (66)$$

if  $\sigma$  is small.

$L$  is the latent heat of vaporization of water.

The vapor pressure after the condensation shock, as has been pointed out, is assumed to be equal to the saturation vapor pressure. Instead of using the exact form of the Clausius-Clapeyron equation which would introduce considerable complexity into the energy equation, a suitable approximation to the actual saturated vapor pressure versus temperature curve was sought which would simplify the solution. If the specific volume of the liquid phase is neglected, the Clausius-Clapeyron equation can be integrated and the relation between the saturated vapor pressure and the temperature may be expressed by a relation of the form:

$$p_{v2} = p_{2\infty} = C \exp\left(\frac{-L m_v}{RT}\right) \quad (67)$$

where the constant  $C$  could be determined by fitting the approximating curve (67) to the actual curve at a particular point. It should be

noted that although the latent heat of vaporization  $L$  is a function of  $T$ , the variation with temperature in a particular range considered is usually not very large and therefore it is possible with only a slight inaccuracy to treat this also as a constant.

The saturated vapor pressure is taken to be 27 mm. Hg or 0.523 p.s.i. at 300°K and a constant value for  $L$  of 560 calories per gram is used. With these numerical values,

$$C = 1.176 \times 10^{17}$$

if  $p_{\infty}$  is measured in p.s.i. Equation (67) is represented by the dotted curve in Fig. (3) while the true saturated vapor pressure versus temperature curve is represented by the solid curve. In this case, for illustrative purposes, the two curves were matched at a temperature of 300°K. The approximation appears to be quite good.

The mixture of water vapor and air is assumed to obey the perfect gas law,

$$\frac{p_2}{p_1} \cdot \frac{\rho_1}{\rho_2} = \frac{T_2}{T_1} \quad (68)$$

Utilizing equation (63), the following result is obtained:

$$\frac{p_2}{p_1} \cdot \frac{u_2}{u_1} = \frac{T_2}{T_1} \quad (69)$$

A combination of the continuity and momentum equations yields the relation:

$$\frac{p_2}{p_1} = 1 + \gamma M_1^2 \left( 1 - \frac{u_2}{u_1} \right) \quad (70)$$

where  $M_1 = \frac{u_1}{a_1}$  is the Mach number before the shock.

Now,

$$\frac{u_2}{u_1} = \frac{M_2}{M_1} \left( \frac{T_2}{T_1} \right)^{1/2} \quad (71)$$

Combining the equations (69), (70) and (71) we obtain the expression relating the pressure jump across the shock to the Mach number change as follows:

$$\frac{p_2}{p_1} = \frac{1 + \gamma M_1^2}{1 + \gamma M_1^2 \left(\frac{M_2}{M_1}\right)^2} \quad (72)$$

Similarly, the temperature change across the shock can be expressed in terms of the Mach number before and after as follows:

$$\frac{T_2}{T_1} = \left[ \frac{1 + \gamma M_1^2}{1 + \gamma M_1^2 \left(\frac{M_2}{M_1}\right)^2} \right]^2 \left(\frac{M_2}{M_1}\right)^2 \quad (73)$$

Since only the continuity and momentum equations have been used thus far, formulae (72) and (73) are identical to those which hold for an ordinary normal shock.

The energy equation may be rewritten in the form:

$$\frac{\gamma-1}{2} M_1^2 + 1 + \frac{(\gamma-1)(\sigma_1 - \sigma_2)L}{a_1^2} = \frac{\gamma-1}{2} \frac{u_2^2}{a_1^2} + \frac{a_2^2}{a_1^2} \quad (74)$$

Now,

$$\frac{u_2^2}{a_1^2} = \frac{u_2^2}{u_1^2} \cdot \frac{u_1^2}{a_1^2} = M_1^2 \left(\frac{M_2}{M_1}\right)^4 \left[ \frac{1 + \gamma M_1^2}{1 + \gamma M_1^2 \left(\frac{M_2}{M_1}\right)^2} \right]^2 \quad (75)$$

and

$$\frac{a_2^2}{a_1^2} = \frac{T_2}{T_1} = \left[ \frac{1 + \gamma M_1^2}{1 + \gamma M_1^2 \left(\frac{M_2}{M_1}\right)^2} \right]^2 \left(\frac{M_2}{M_1}\right)^2 \quad (76)$$

Combining equations (75) and (76) with the energy equation (74), we have the following result:

$$\frac{(\gamma-1)(\sigma_1-\sigma_2)L}{a_1^2} = \left(\frac{M_2}{M_1}\right)^2 \left[ \frac{1+\gamma M_1^2}{1+\gamma M_1^2 \left(\frac{M_2}{M_1}\right)^2} \right]^2 \left[ 1 + \frac{\gamma-1}{2} M_1^2 \left(\frac{M_2}{M_1}\right)^2 \right] - \frac{\gamma-1}{2} M_1^2 - 1 \quad (77)$$

The specific humidity after the condensation shock, namely  $\sigma_2$ , can be expressed in terms of the temperature and pressure after the shock by use of equations (59) and (67).

$$\sigma_2 = \frac{C e^{-\frac{L m_v}{RT_2}}}{p_2(k+1) - k C e^{-\frac{L m_v}{RT_2}}} \quad (78)$$

Now, from equation (73)

$$\frac{L m_v}{RT_2} = \frac{L m_v}{RT_1} \left[ \frac{1+\gamma M_1^2 \left(\frac{M_2}{M_1}\right)^2}{1+\gamma M_1^2} \right]^2 \left(\frac{M_1}{M_2}\right)^2 \quad (79)$$

From equation (59) and (72).

$$p_2(k+1) = \frac{(1+\gamma M_1^2)(k+1)}{1+\gamma M_1^2 \left(\frac{M_2}{M_1}\right)^2} \cdot \frac{p_{v1}(k\sigma_1+1)}{\sigma_1(k+1)} \quad (80)$$

where  $p_{v1}$  = vapor pressure before condensation shock.

The specific humidity after the shock,  $\sigma_2$ , can therefore be expressed in terms of the conditions before the shock and the Mach number change across the shock by combining equations (78), (79) and (80).

The energy equation may now be written in terms of only the Mach number change across the shock and the initial conditions.

$$\begin{aligned}
& \left(\frac{M_2}{M_1}\right)^2 \left[ \frac{1 + \delta M_1^2}{1 + \delta M_1^2 (M_2/M_1)^2} \right]^3 \left[ 1 + \frac{\delta-1}{2} M_1^2 \left(\frac{M_2}{M_1}\right)^2 \right] \frac{p_{v_1} (k\sigma_1 + 1)}{\sigma_1} \\
& - \left[ 1 + \frac{\delta-1}{2} M_1^2 \right] \left[ \frac{1 + \delta M_1^2}{1 + \delta M_1^2 (M_2/M_1)^2} \right] \frac{p_{v_1} (k\sigma_1 + 1)}{\sigma_1} \\
& - \frac{(\delta-1) m_a L}{\delta R T_1} \left[ \frac{1 + \delta M_1^2}{1 + \delta M_1^2 (M_2/M_1)^2} \right] p_{v_1} (k\sigma_1 + 1) \quad (81) \\
& = \left\{ k \left(\frac{M_2}{M_1}\right)^2 \left[ \frac{1 + \delta M_1^2}{1 + \delta M_1^2 (M_2/M_1)^2} \right]^2 \left[ 1 + \frac{\delta-1}{2} M_1^2 \left(\frac{M_2}{M_1}\right)^2 \right] - k \left[ 1 + \frac{\delta-1}{2} M_1^2 \right] \right. \\
& \quad \left. - \frac{(k\sigma_1 + 1)(\delta-1) m_a L}{\delta R T_1} \right\} C e^{-\frac{L m_v}{R T_1} \left[ \frac{1 + \delta M_1^2 \left(\frac{M_2}{M_1}\right)^2}{1 + \delta M_1^2} \right] \left(\frac{M_1}{M_2}\right)^2}
\end{aligned}$$

A simplification is obtained by taking the logarithm of both sides:

$$\begin{aligned}
& \ln \frac{\left(\frac{M_2}{M_1}\right)^2 \left[ \frac{1 + \delta M_1^2}{1 + \delta M_1^2 (M_2/M_1)^2} \right]^2 \left[ 1 + \frac{\delta-1}{2} M_1^2 \left(\frac{M_2}{M_1}\right)^2 \right] - \left[ 1 + \frac{\delta-1}{2} M_1^2 \right] - \left[ \frac{\delta-1}{\delta R T_1} m_a L \frac{(k\sigma_1 + 1)}{k} \right]}{\left(\frac{M_2}{M_1}\right)^2 \left[ \frac{1 + \delta M_1^2}{1 + \delta M_1^2 (M_2/M_1)^2} \right]^2 \left[ 1 + \frac{\delta-1}{2} M_1^2 \left(\frac{M_2}{M_1}\right)^2 \right] - \left[ 1 + \frac{\delta-1}{2} M_1^2 \right] - \left[ \frac{\delta-1}{\delta R T_1} m_a L \sigma_1 \right]} \quad (82) \\
& = \frac{L m_v}{R T_1} \left[ \frac{1 + \delta M_1^2 \left(\frac{M_2}{M_1}\right)^2}{1 + \delta M_1^2} \right] \left(\frac{M_1}{M_2}\right)^2 + \ln \frac{1 + \delta M_1^2}{1 + \delta M_1^2 (M_2/M_1)^2} \\
& \quad + \ln \left[ \frac{p_{v_1} (k\sigma_1 + 1)}{C k \sigma_1} \right]
\end{aligned}$$

Let us consider specifically the last term in the energy equation,

(82):

$$\ln \frac{p_v(k\sigma_i+1)}{Ck\sigma_i} = \ln \frac{p_{v1}}{C} + \ln \frac{k\sigma_i+1}{k\sigma_i} \quad (83)$$

Now,

$$(p_\infty)_{T=T_1} = p_{1\infty} = C e^{-\frac{Lm_v}{RT_1}} \quad (84)$$

Therefore,

$$\ln \frac{p_{v1}}{C} + \ln \frac{k\sigma_i+1}{k\sigma_i} = \ln \left[ \frac{p_{v1}}{p_{1\infty}} e^{-\frac{Lm_v}{RT_1}} \right] + \ln \frac{k\sigma_i+1}{k\sigma_i} \quad (85)$$

$$= \ln \frac{p_{v1}}{p_{1\infty}} - \frac{Lm_v}{RT_1} + \ln \frac{k\sigma_i+1}{k\sigma_i} \quad (86)$$

But the supersaturation pressure ratio  $\ln \frac{p_{v1}}{p_{1\infty}}$  is dependent only on temperature  $T_1$  from Fig. (2), so that if the initial temperature and the specific humidity are given, the quantities in equation (86) are determined.

Equation (82) may now be more conveniently written in the form:

$$\ln \frac{\left(\frac{M_2}{M_1}\right)^2 \left[ \frac{1+\delta M_1^2}{1+\delta M_1^2 \left(\frac{M_2}{M_1}\right)^2} \right]^2 \left[ \frac{1+\frac{\delta-1}{2} M_1^2 \left(\frac{M_2}{M_1}\right)^2}{1+\frac{\delta-1}{2} M_1^2} \right] - \left[ \frac{\delta-1}{\delta RT_1} m_a L \frac{(k\sigma_i+1)}{k} \right]}{\left(\frac{M_2}{M_1}\right)^2 \left[ \frac{1+\delta M_1^2}{1+\delta M_1^2 \left(\frac{M_2}{M_1}\right)^2} \right]^2 \left[ \frac{1+\frac{\delta-1}{2} M_1^2 \left(\frac{M_2}{M_1}\right)^2}{1+\frac{\delta-1}{2} M_1^2} \right] - \left[ \frac{\delta-1}{\delta RT_1} m_a L \sigma_i \right]} \quad (87)$$

$$= \ln \left[ \frac{1+\delta M_1^2}{1+\delta M_1^2 \left(\frac{M_2}{M_1}\right)^2} \right] + \ln \frac{p_{v1}}{p_{1\infty}} + \ln \frac{k\sigma_i+1}{k\sigma_i}$$

$$+ \frac{Lm_v}{RT_1} \left\{ \left[ \frac{1+\delta M_1^2 \left(\frac{M_2}{M_1}\right)^2}{1+\delta M_1^2} \right] \left(\frac{M_1}{M_2}\right)^2 - 1 \right\}$$

Symbolically, this last equation can be written:

$$\frac{M_2}{M_1} = F(M_1, T_1, \sigma_1) \quad (88)$$

It may be solved by a method of successive approximations and a set of charts can thus be obtained. For illustrative purposes, these computations have been carried out for  $M_1 = 1.3, 2.0, 3.0, 3.5,$  and  $4.0$  and  $T_1 = 250^\circ\text{K}, 270^\circ\text{K}, 300^\circ\text{K}, 320^\circ\text{K}$  and  $350^\circ\text{K}$ . These charts have been constructed for the range  $0 < \sigma_1 < 0.1$  and are shown in Figures 7 to 11 inclusive. Cross plots of some of this data in order to more clearly illustrate variations with temperature are shown in Figs. (12) to (17). For much higher values of  $\sigma$ , the results using formula (87) would be questionable since the water vapor content would then be such as to invalidate the present theory inasmuch as the total energy of the liquid phase would have to be included in the energy equation and the simplified expressions for the velocity of sound in the mixture would have to be modified.

For a qualitative study of the behavior of the curves for higher values of  $\sigma$ , the computations were also carried out up to the maximum strength of shock possible in all cases, that is,  $M_2 = 1$ . The qualitative data are shown in Figs. (18) to (22) inclusive. It should be emphasized, however, that these curves have no quantitative significance for high values of  $\sigma$ .

In actual aeronautical applications, the specific humidity is usually considerably less than 0.1 so that it may be stated that the assumptions of the present theory are quite satisfactory for such usage.



Once the Mach number change across the shock wave has been determined, the pressure and temperature changes can be computed readily by means of equations (72) and (73) respectively or by using Figs. (23) and (24). The latter figures are merely the plot of equations (72) and (73).

In the above calculations it is noted that the strongest condensation shock possible is indicated as one in which the Mach number after the shock drops to unity. The question then naturally arises as to why a jump from a supersonic velocity to a subsonic velocity is not possible. Equation (87) has two roots, so that the plot of  $\sigma$  versus  $\frac{M_2}{M_1}$  has two branches: the branch which would entail a jump from a supersonic velocity to a subsonic velocity is shown for a special case in Figure 22 as a dotted curve. It can be proved, however, that such a transition is not possible with a monotonic addition of heat as is the case in a condensation process. Therefore, the only possible type of condensation shock is one entailing a change from one supersonic velocity to another lower supersonic velocity, in other words, only one branch of the curve expressing the relationship between the specific humidity and the Mach number ratio,  $\frac{M_2}{M_1}$ , has physical significance. In order to see this let us consider the fundamental fluid flow equations with heat addition.

1) Continuity

$$d(\rho u) = 0 \quad (89)$$

2) Energy

$$d \left( \frac{u^2}{2} + c_p T \right) = dh \quad (90)$$

3) Momentum

$$\rho u du = - dp \quad (91)$$

4) Equation of state

$$p = \rho \frac{R}{m} T \quad (92)$$

From these expressions it is easily deduced that:

$$u du = \frac{\gamma-1}{M^2-1} dh \quad (93)$$

If the Mach number  $M$  is supersonic, then it is clear from the above relation that addition of heat or a positive value for  $dh$  will result in a decrease in the velocity. If the Mach number is subsonic, then an addition of heat will result in an increase in velocity. Hence, it is clearly not possible to go from a supersonic speed to a subsonic by a monotonic heat input as in a condensation process.

The general one-dimensional theory of steady compressible fluid flow considering friction and head addition has recently (Ref. 26) been summarized in a rather neat manner using  $1-M$  as the basic parameter and formulating the general problem as a set of three simultaneous equations. Steady-state solutions exist in all cases where the determinant of the variable parameters is different from zero. This determinant is only zero when  $1-M = 0$ .

The particular conclusion that unity is the lowest possible Mach number that can be reached in a supersonic stream by a monotonic head addition process, such as a condensation shock is, of course, verified as a special case.

V. POSSIBILITY OF CONTINUOUS CONDENSATION IN A STREAM OF HIGH WATER CONTENT

From the above considerations, the question naturally arises as to what would happen if at a given temperature  $T$ , and Mach number  $M$ , where the critical supersaturation conditions are reached, the specific humidity is higher than the value which, from the previous analysis, would cause a condensation shock of such strength that the Mach number after the shock would be unity. In this case, a shock would presumably occur which would cause the Mach number to drop to unity after the shock, but now the mixture would still be supersaturated. Let us now consider the fundamental flow equations for a non-constant cross-section. In this case the continuity equation is modified, to include the change in cross-sectional area,  $df$ , that is:

$$d(\rho u f) = 0 \quad (94)$$

From the energy equation and the equation of state we have,

$$u du + \frac{\gamma}{\gamma-1} \frac{dp}{\rho} - \frac{\gamma}{\gamma-1} \frac{p}{\rho} \frac{d\rho}{\rho} = dh \quad (95)$$

Utilizing the continuity and momentum equations, this may be written in the form:

$$u du - \frac{\gamma}{\gamma-1} u du + \frac{a^2}{\gamma-1} \left[ \frac{du}{u} + \frac{df}{f} \right] = dh \quad (96)$$

$$u du \left[ \frac{1-M^2}{(\gamma-1)M^2} \right] + \frac{a^2}{\gamma-1} \frac{df}{f} = dh \quad (97)$$

An examination of equation (97) clearly illustrates that for a constant cross-section no heat addition is possible if the Mach number is unity. However, on the basis of the present calculations, if a change in cross-sectional area occurs, then it is possible to add more heat and this heat addition, furthermore, will be a maximum if the

Mach number is maintained as unity. It is possible, therefore, that in the case where a supersaturated mixture exists at a Mach number of unity, then further condensation will occur only if the cross-sectional area changes and then heat will be released or condensation will occur in a manner such that the velocity will be maintained equal to the velocity of sound, that is,

$$\frac{dh}{df} = \frac{a^2}{(\gamma-1)f} \quad (98)$$

Thus, if the cross-sectional area distribution is given, the quantity of heat released by condensation,  $dh$ , can be calculated as a function of the change in area,  $df$ . In this way condensation will occur in a continuous manner until saturation conditions are achieved. If there is no change in area, then the one-dimensional considerations yield the result that no heat can be absorbed by a stream of fluid flowing at a Mach number of unity.

It is interesting to consider the special gas law which the mixture would observe under such conditions. From the equation of momentum (91):

$$-\frac{dp}{\rho} = u du$$

Since, under conditions of continuous condensation, the velocity of the fluid is maintained equal to that of the sound propagation velocity in the original water vapor and air mixture, the following relation holds:

$$u^2 = \frac{\gamma p}{\rho} \quad (99)$$

Therefore,

$$2u du = \frac{\gamma}{\rho} dp - \frac{\gamma p}{\rho} \frac{d\rho}{\rho} \quad (100)$$

Utilizing equations (91) and (100), the following relationship between the pressure and the density in the continuous condensation zone is obtained.

$$\frac{dp}{p} = \frac{\gamma}{\gamma+2} \frac{d\rho}{\rho} \quad (101)$$

or

$$p = k \rho^{\frac{\gamma}{\gamma+2}} \quad (102)$$

It is interesting to calculate the propagational velocity of sound,  $a_c$ , in this continuous condensation zone.

$$a_c^2 = \frac{dp}{d\rho} = k \frac{\gamma}{\gamma+2} \rho^{-2/\gamma+2} \quad (103)$$

or

$$a_c^2 = \frac{\gamma}{\gamma+2} \frac{p}{\rho} \quad (104)$$

The actual velocity of the mixture in this region, however, is equal to  $\frac{\gamma p}{\rho}$ . Therefore, the true Mach number,  $M_c$ , expressed in terms of the true sound propagation velocity, is given by the expression,

$$M_c^2 = \frac{u^2}{a_c^2} = \gamma+2 \quad (105)$$

If the specific humidity is relatively low, the value of  $\gamma$ , the ratio of the specific heats, is approximately 1.4 and hence, the rather interesting result is obtained that a continuous condensation region is, strictly speaking, a supersonic stream whose Mach number  $M_c = \sqrt{\gamma+2} \cong 1.84$ .

It should be emphasized that the above considerations are valid only for one-dimensional flow. In order to ascertain under what conditions a continuous condensation region could exist in a two-dimensional flow, it would require a considerably more detailed consideration.

It has been shown that, under certain conditions, in a one-dimensional supersonic flow, a condensation shock can occur which will be followed by a zone of continuous condensation. The velocity of the fluid in this zone, furthermore, is maintained at a value equal to the sound propagational velocity in the original stream, or, expressed in terms of conditions in the continuous condensation region, the velocity is maintained at a value such that the true Mach number of the flow is equal to  $M_c = \sqrt{\gamma + 2}$ .

The existence of such a zone has been shown to be possible. Careful experimentation, however, will be necessary to establish whether such conditions are actually found to exist or whether, because of stability considerations, such a state is not attainable but instead the flow breaks down with a resultant non-stationary condensation shock.

It is interesting to consider, however, the possible development of such a zone because of the rather interesting property that it behaves like a supersonic stream with Mach number,  $M_c = \sqrt{\gamma + 2}$ .

## VI. PROCEDURE OF COMPUTATIONS

It might be of assistance to briefly tabulate the steps in investigating the occurrence and strength of a normal condensation shock using the simplified theory presented above. Suppose that it is desired to ascertain the location and strength of a condensation shock in a supersonic wind tunnel. The procedure may be outlined as follows:

- i) Determine the stagnation pressure and dew point of the mixture of air and water vapor. Use Fig. (5) to establish the specific humidity.
- ii) From the fundamental equations of gas dynamics, the pressure, temperature and density at the throat of the wind tunnel are related to the stagnation pressure and temperature by the relations:

$$T_t = \frac{2}{\gamma+1} T_0 \quad (106)$$

$$p_t = \left(\frac{2}{\gamma+1}\right)^{\frac{\gamma}{\gamma-1}} p_0 \quad (107)$$

If  $f_t$  is the throat area and  $f_x$  the area at any section  $x$  downstream of the throat, then the quantities  $T_x$  and  $p_x$ , may be related to the stagnation conditions by the following relations:

$$\frac{f_x}{f_t} = \sqrt{\frac{\gamma-1}{2}} \left(\frac{2}{\gamma+1}\right)^{\frac{\gamma+1}{2(\gamma-1)}} \frac{1}{\left(\frac{T_x}{T_0}\right)^{\frac{1}{\gamma-1}} \sqrt{1 - \frac{T_x}{T_0}}} \quad (108)$$

$$\frac{f_x}{f_t} = \sqrt{\frac{\gamma-1}{2}} \left(\frac{2}{\gamma+1}\right)^{\frac{\gamma+1}{2(\gamma-1)}} \frac{1}{\left(\frac{p_x}{p_0}\right)^{\frac{1}{\gamma}} \sqrt{1 - \left(\frac{p_x}{p_0}\right)^{\frac{\gamma-1}{\gamma}}}} \quad (109)$$

If it is preferable to express  $T_x$  and  $p_x$  in terms of conditions at the throat, the following relations hold:

$$\frac{f_x}{f_t} = \sqrt{\frac{\delta-1}{2}} \frac{1}{\left(\frac{T_x}{T_t}\right)^{\frac{1}{\delta-1}} \sqrt{\frac{\delta+1}{2} - \frac{T_x}{T_t}}} \quad (110)$$

$$\frac{f_x}{f_t} = \sqrt{\frac{\delta-1}{2}} \frac{1}{\left(\frac{p_x}{p_t}\right)^{\frac{1}{\delta}} \sqrt{\frac{\delta+1}{2} - \left(\frac{p_x}{p_t}\right)^{\frac{\delta-1}{\delta}}}} \quad (111)$$

The Mach number at the section  $x$  can be related to the area ratio according to the following expression:

$$\frac{f_x}{f_t} = \frac{1}{M_x} \left[ \frac{2}{\delta+1} \left( 1 + \frac{\delta-1}{2} M_x^2 \right) \right]^{\frac{\delta+1}{2(\delta-1)}} \quad (112)$$

Charts expressing the relationships (110) to (112) may be constructed and used to determine the Mach number, temperature and pressure at any section downstream of the throat. These are shown in Fig. (25).

- iii) Since the total pressure is known at every section and the specific humidity of the mixture has been determined, the vapor pressure at every section can be obtained from equation (62) or Fig. (6).
- iv) The temperature at every section is known and therefore the value of the saturation vapor pressure is known from Fig. (3). Hence it is possible to calculate  $\ln \frac{P_v}{P_\infty}$  at every section.
- v) If the temperature  $T$  is plotted versus this quantity  $\ln \frac{P_v}{P_\infty}$ , then condensation will occur when this curve intersects the critical supersaturation curve, Fig. (2). This establishes the location of the condensation shock.



- vi) From equations (110), (111) and (112) the temperature, pressure and Mach number at this section are known.
- vii) From other charts similar to those shown in Figs. (7) to (11), or from equation (87), the change in Mach number across the shock is determined and the pressure and temperature changes across the shock then follow from Figs. (23) and (24) respectively.

## VII. ILLUSTRATIVE EXAMPLE

In order to better illustrate the computation procedure, it may be well to consider a simple example. For this purpose, suppose that it is desired to ascertain the location and strength of a condensation shock in a supersonic wind tunnel nozzle of rectangular cross-section.

Suppose the nozzle angle for this particular nozzle is  $16^\circ$ .

The following notation is used:

$d_t$  = height of throat section

$t$  = width of throat section (assumed constant)

$d_x$  = height at section  $x$  downstream of throat

$$\frac{f_x}{f_t} = \frac{d_x}{d_t} = 1 + \alpha_x \tan 8^\circ \quad (113)$$

where

$$\alpha_x = \frac{2x}{d_t} \quad (114)$$

The stagnation conditions were assumed as follows:

$$p_0 = 450 \text{ mm. Hg.}$$

$$\text{Dew point} = 30^\circ\text{C.}$$

$$T_0 = 450^\circ\text{K.}$$

- i) From formula (59) or Fig. (5), the specific humidity,  $\sigma$ , can be determined. This is found to be 0.0455.
- ii) From charts expression the relationships (110), (111) and (112), that is, Fig. (25), the pressure, temperature and Mach number were computed for various values of  $\alpha_x$ .
- iii) From equation (62), the vapor pressure was also computed as a function of  $\alpha_x$ .
- iv) The saturation vapor pressure as a function of  $\alpha_x$  was determined by use of Fig. (3) and the temperature distribution computed under (ii).

v) The quantity  $\ln \frac{P_v}{P_\infty}$  was computed and a plot of the absolute temperature,  $T$ , versus  $\ln \frac{P_v}{P_\infty}$  was plotted for increasing  $\alpha_x$ . This is indicated by the dotted line in Fig. (26). A replot of the theoretical critical supersaturation curve is shown here for convenience. It has also been extended to cover the lower temperature range necessary. The intersection of these two curves gives the temperature before the condensation shock,  $T_1$ . This is seen to be  $247.5^\circ \text{K}$ ; a plot of  $\ln \frac{P_v}{P_\infty}$  versus  $\alpha_x$  is shown in Fig. (27).

vi) The following results are then obtained for the location of the shock and the conditions before the shock.

$$\alpha_x = \frac{2x}{d_t} = 5.08$$

$$T_1 = 247.5^\circ \text{K}$$

$$P_1 = 56.5 \text{ mm. Hg.}$$

$$M_1 = 2.01$$

vii) Equation (87) can now be used to determine the change in Mach number across the shock and then the pressure jump and temperature jump follow immediately from equations (72) and (73). The results are:

$$\frac{T_2}{T_1} = 1.793$$

$$\frac{P_2}{P_1} = 2.362$$

$$\frac{M_2}{M_1} = 0.567$$

or with the given initial values:

$$T_2 = 444.0^\circ\text{K}$$

$$p_2 = 133.7 \text{ mm. Hg.}$$

$$M_2 = 1.14$$

To estimate the effectiveness of the theoretical critical supersaturation curve obtained under the present considerations, the calculations for this illustrative example were repeated using the empirical critical supersaturation curve.

The following results were obtained for the location of the shock and the conditions before the shock:

$$d_x = \frac{2x}{d_t} = 4.68.$$

$$T_1 = 252.2^\circ\text{K.}$$

$$p_1 = 60.38 \text{ mm. Hg.}$$

$$M_1 = 1.97.$$

The change in temperature, pressure, and Mach number across the condensation shock was found to be:

$$\frac{T_2}{T_1} = 1.739$$

$$\frac{p_2}{p_1} = 2.266$$

$$\frac{M_2}{M_1} = 0.582$$

The conditions after the shock are therefore:

$$T_2 = 438.6^\circ\text{K}$$

$$p_2 = 136.8 \text{ mm. Hg.}$$

$$M_2 = 1.15$$

It is noted that the agreement is quite good.

VIII. OBLIQUE SHOCK WAVES

With small modification, the results derived for the case of normal condensation shocks can be applied to the case of oblique condensation shocks.

Suppose that the incident velocity of the mixture of air and water vapor before the shock is  $w_1$ . (Fig. 23). Let  $\alpha$  be the angle of inclination of the condensation shock to the direction of the fluid flow. If  $u_1$  and  $v_1$  are the components of  $w_1$  normal and parallel to the shock, clearly:

$$u_1 = w_1 \sin \alpha \quad (115)$$

$$v_1 = w_1 \cos \alpha \quad (116)$$

Let  $w_2$  be the fluid velocity after the shock with component  $u_2$  normal to the shock and  $v_2$  parallel to the shock.

$$u_2 = w_2 \sin \beta \quad (117)$$

$$v_2 = w_2 \cos \beta \quad (118)$$

From ordinary oblique shock theory, by momentum considerations:

$$v_1 = v_2$$

Therefore,

$$\frac{u_2}{u_1} = \frac{w_2 \sin \beta}{w_1 \sin \alpha} = \frac{v_2}{v_1} \frac{\cos \alpha}{\cos \beta} \cdot \frac{\sin \beta}{\sin \alpha} = \frac{\tan \beta}{\tan \alpha} \quad (119)$$

Let  $M_1$  be the Mach number of the component of the fluid stream normal to the condensation shock and let  $M_2$  be the Mach number of the normal component after the shock. Then:

$$\frac{M_2}{M_1} = \frac{\tan \beta}{\tan \alpha} \cdot \left( \frac{T_1}{T_2} \right)^{1/2} \quad (120)$$

and using equation (73), we obtain the result:

$$\left(\frac{M_2}{M_1}\right)^2 \left[ \frac{1 + \gamma M_1^2}{1 + \gamma M_1^2 (M_2/M_1)^2} \right] = \frac{\tan \beta}{\tan \alpha} \quad (121)$$

or,

$$\left(\frac{M_2}{M_1}\right)^2 = \frac{\tan \beta}{\tan \alpha + \gamma M_1^2 [\tan \alpha - \tan \beta]} \quad (122)$$

Now, for a given  $M_1$ ,  $T_1$ ,  $\sigma_1$ , the change in Mach number across a normal shock is known from the results of section IV. Therefore, for a given angle of inclination  $\alpha$ , of an oblique condensation shock wave, the angle of turn of the fluid stream,  $\alpha - \beta$ , caused by the shock can be determined from equation (122). Charts have been drawn up for the same particular cases as were treated in the study of normal shock waves to express the angle of turn  $\alpha - \beta$ , in terms of the angle of inclination of the shock,  $\alpha$ , for various values of  $\frac{M_2}{M_1}$ . These are shown in Figs. (29) to (33) inclusive. It should be emphasized that in these charts the Mach numbers are those of the components of the fluid stream normal to the condensation shock.

## IX. APPLICATIONS

In order to utilize the results of the previous section it is first necessary to have a complete knowledge of the two-dimensional flow field. If this is known, the locus of points at which critical supersaturation conditions are realized determines the form of the condensation shock and the angle  $\alpha$ . The results of the previous section can then be readily applied.

In the case of flow through supersonic nozzles, various investigators (Ref. 27, 28, 29, 30) have obtained two-dimensional solutions applicable in the vicinity of the throat. The Taylor solutions are of the symmetrical type, that is, two supersonic regions first appear at the walls of the throat and grow with increasing mass flow. There is, however, a limit to the size of these symmetrical supersonic regions. This limit depends upon the ratio of the radius of curvature of the throat section to the diameter of the throat. A transition to the unsymmetrical Meyer type solution then presumably occurs and the flow becomes supersonic after the throat section. The use of these two-dimensional theories in the present problem is highly limited since the standard method has been to use a series expansion for the velocity potential and so the results are confined to the immediate vicinity of the throat where a reasonable rate of convergence of the series occurs. Since, except in very special cases, the critical supersaturation conditions will not occur in the immediate vicinity of the throat, the applicability of the above theories is not extensive. Numerical methods (Ref. 31) can, however, be effectively applied.

For general two-dimensional transonic flow, the flow field can be determined by either the analytical method (Ref. 32) or by the numerical method (Ref. 33).

Once this is done, however, the critical supersaturation curve can be used to determine the shape of the condensation shock. After this pattern is known, the results of the present investigation can be immediately applied for the determination of conditions after the shock and the resulting flow field.

As has been emphasized, condensation shocks can have a very dominant influence on airfoil characteristics at high speeds. Their influence in steam turbines has been noted and other related applications may require a further knowledge of their effect and behavior. The rapid development of high speed aircraft and missiles has made the problem one of possible importance and systematic experimental studies would certainly be worthwhile from the standpoint of extending the present rather scanty knowledge of this phenomenon. It is interesting to note that Ackeret (Ref. 34) under certain conditions, has encountered a "double" shock, which he suggests may be composed of a condensation shock followed immediately by an ordinary shock. The possibility of such a process is clearly brought out in the present analysis. Referring once again to Fig. (22), it is clear that the solid curve is representative of the first, or condensation shock, while the dotted curve is representative of the second, or ordinary shock. At a specific humidity corresponding to the junction of the two branches, the "double" shock should merge into a single shock while for higher humidities, the present theoretical investigation would



indicate the formation of a possible continuous condensation zone or else the appearance of a non-stationary condensation shock.

REFERENCES

1. Lord Rayleigh: "On the Discharge of Gases Under High Velocity". Phil. Mag. (6), 32 (1916), p. 177.  
"Flow of Compressible Fluid Past an Obstacle". Phil. Mag. (6), 32 (1916).
2. B. Riemann: "Über die Fortpflanzung ebener Luftwellen von endlicher Schwingungsweite". Abh. d. Gesell. d. Wissen, Göttingen, Math. - Physik Kl., 8 (1860).
3. A. Hugoniot: Comptes rendus, 103 (1886) p. 1178. Journal école polyt., Cah. 58 (1888).
4. S. Tschaplygin: "Gas Jets". Scientific Memoirs, Moscow University (1902).
5. L. Prandtl: "Über Strömungen, deren Geschwindigkeiten mit der Schallgeschwindigkeit vergleichbar sind". Journal of the Aero Research Institute, Tokyo Imperial University, 65 (1930) p. 14.
6. Th. von Kármán: "The Problem of Resistance in Compressible Fluids". Proceedings of the Volta High Speed Conference, Rome (1935) p. 197.
7. J. Ackeret: "Luftkräfte auf Flügel, die mit grösserer als Schallgeschwindigkeit bewegt werden". Z.F.M., 16 (1925) p. 72.
8. G. I. Taylor: "Recent Works on the Flow of Compressible Fluids". Journal of the London Math. Soc., Vol. 5 (1930) p. 224.
9. A. Büsemann: "Drücke auf kegelförmige Spitzen bei Bewegung mit Überschallgeschwindigkeit". Z.A.M.M. Vol. 9 (1929) p. 496.
10. H. S. Tsien and A. Fejér: "A Method for Predicting the Transonic Flow over Airfoils and Similar Bodies for Data Obtained at Small Mach Numbers". GALCIT Report to AAF Materiel Command (1945).
11. L. Prandtl: "Allgemeine Überlegungen über die Strömung zusammen-drückbarer Flüssigkeiten". Proceedings of the Volta High Speed Conference, Rome (1935), p. 197.
12. R. Hermann: "Der Kondensationsstos in Überschall-Windkanaldüsen". Z.A.M.M., Vol. 19 (1942) p. 201.
13. K. Oswatitsch: "Kondensationerscheinungen in Überschallendüsen". Z.A.M.M., Vol. 22 (1942) p. 1, française 63 (1866) p. 1144.
14. Hirn and Cazin: Comptes rendus de l'Académie française 63 (1866) p. 1144.
15. J. I. Yellott: "Supersaturated Steam". Engineering, Vol. 137 (1934) p. 303. "Condensation of Flowing Steam", Engineering, Vol. 143 (1937) p. 647.

16. A. Stodola: "Dampf-und Gasturbinen". (1924), p. 118.
17. A. M. Binnie: "The Pressure Distribution in a Convergent-Divergent Steam Nozzle". Inst. of Mech. Engineers, Vol. 138, p. 229.
18. W. Thomson: Proceedings of the Royal Society Edinburgh, Vol. 7 (1870).
19. M. Volmer and A. Weber: Keimbildung in übersättigten Gebilden". Zeitschrift für physikalische Chemie. Vol. 119 (1926).
20. L. Farkas: "Keimbildungsgeschwindigkeit in übersättigten Dämpfen". Zeitschrift für physikalische Chemie, Vol. 125 (1927).
21. I. Stranski and R. Kaischew: "Zur kinetischen Ableitung der Keimbildungsgeschwindigkeit". Zeitschrift für physikalische Chemie, Abt. B., Vol. 26 (1934).
22. R. Becker and W. Döring: "Kinetische Behandlung der Keimbildung in übersättigten Dämpfen". Annalen der Physik, Vol. 24 (1936).
23. A. Sander and G. Damköhler: "Übersättigung bei der spontanen Keimbildung in Wasserdampf". Naturwissenschaften. Vol. 31, No. 39/40, (1943), p. 460.
24. H.-W. Liepmann and A. Puckett: "Introduction to Aerodynamics of a Compressible Fluid". John Wiley and Sons. (1946).
25. Smithsonian Meteorological Tables pp. 180-201. Fifth Revised Edition (1931).
26. B. Hicks, D. Montgomery, R. Wasserman: "The One-Dimensional Theory of Steady Compressible Fluid Flow in Ducts With Friction and Heat Addition". N.A.C.A. Adv. Restricted Report. No. E6E22, (1946).
27. Th. Meyer: "Über Zweidimensionale Berwegungsvorgänge in einem Gas, das mit Überschallgeschwindigkeit strömt". Göttingen Dissertation (1907).
28. G. I. Taylor: "The Flow of Air at High Speeds Past Curved Surfaces". R. and M. 1381 (1930).
29. H. Görtler: "Zum Übergang von Unterschall- zu Überschallgeschwindigkeiten in Düsen". Z.A.M.M. Vol. 19 (Dec. 1939).
30. K. Oswatitsch and W. Rothstein: "Das Strömungsfeld in einer Lavaldüse". pp. 1-91 to 1-102, Jahrbuch der deutschen Luftfahrtforschung, (1942).

31. H. W. Emmons: "The Theoretical Flow of a Frictionless, Adiabatic, Perfect Gas Inside of a Two-Dimensional Hyperbolic Nozzle". N.A.C.A. Technical Note No. 1003.
32. H. S. Tsien and Y. H. Kuo: "Two-Dimensional Irrotational Mixed Subsonic and Supersonic Flow of a Compressible Fluid and the Upper Critical Mach Number". GALCIT Report to N.A.C.A. (1945).
33. H. W. Emmons: "The Numerical Solution of Compressible Fluid Flow Problems". N.A.C.A. Technical Note No. 932 (May 1944).
34. J. Ackeret, F. Feldmann and N. Rott: "Untersuchungen an Verdichtungsstößen und Grenzschichten in schnell bewegten Gasen". Mitteilungen aus dem Institut für Aerodynamik, Nr. 10 (1946).



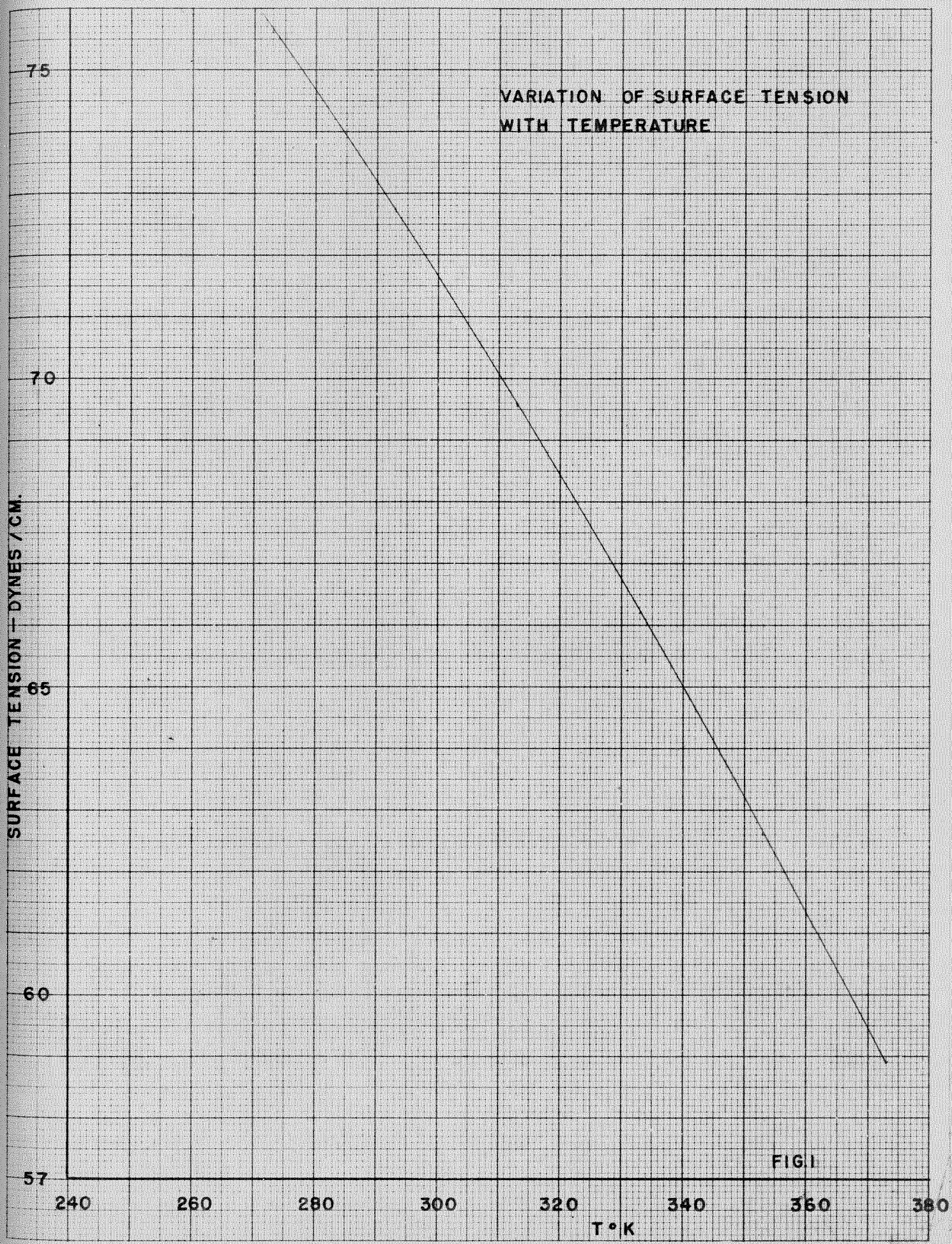


FIG. 1



RELATIONSHIP BETWEEN TEMPERATURE  
AND MAXIMUM SUPERSATURATION FOR  
MIXTURE OF AIR AND WATER VAPOR.

$p_v$  = VAPOR PRESSURE

$p_{\infty}$  = SATURATED VAPOR PRESSURE

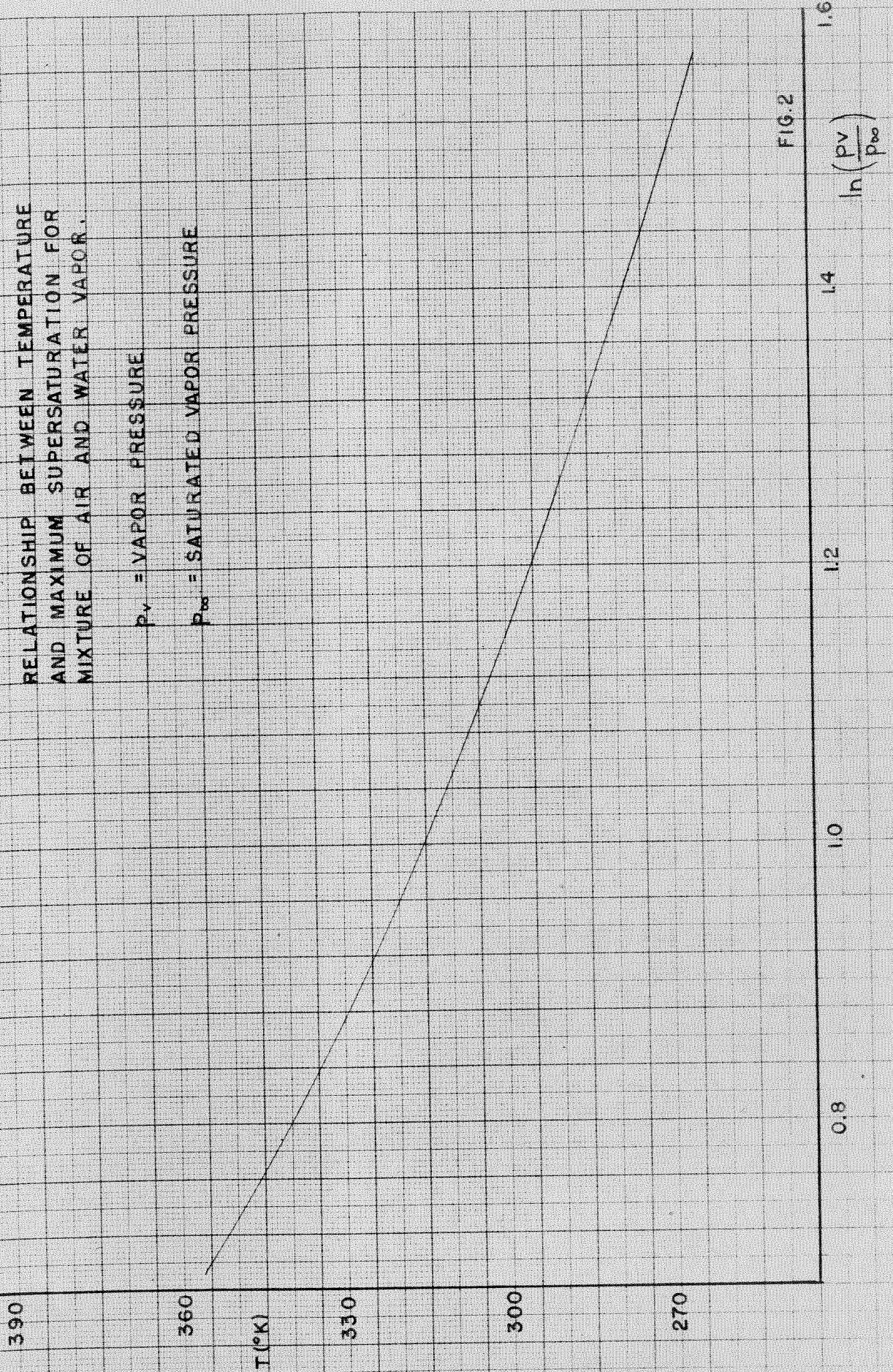


FIG. 2



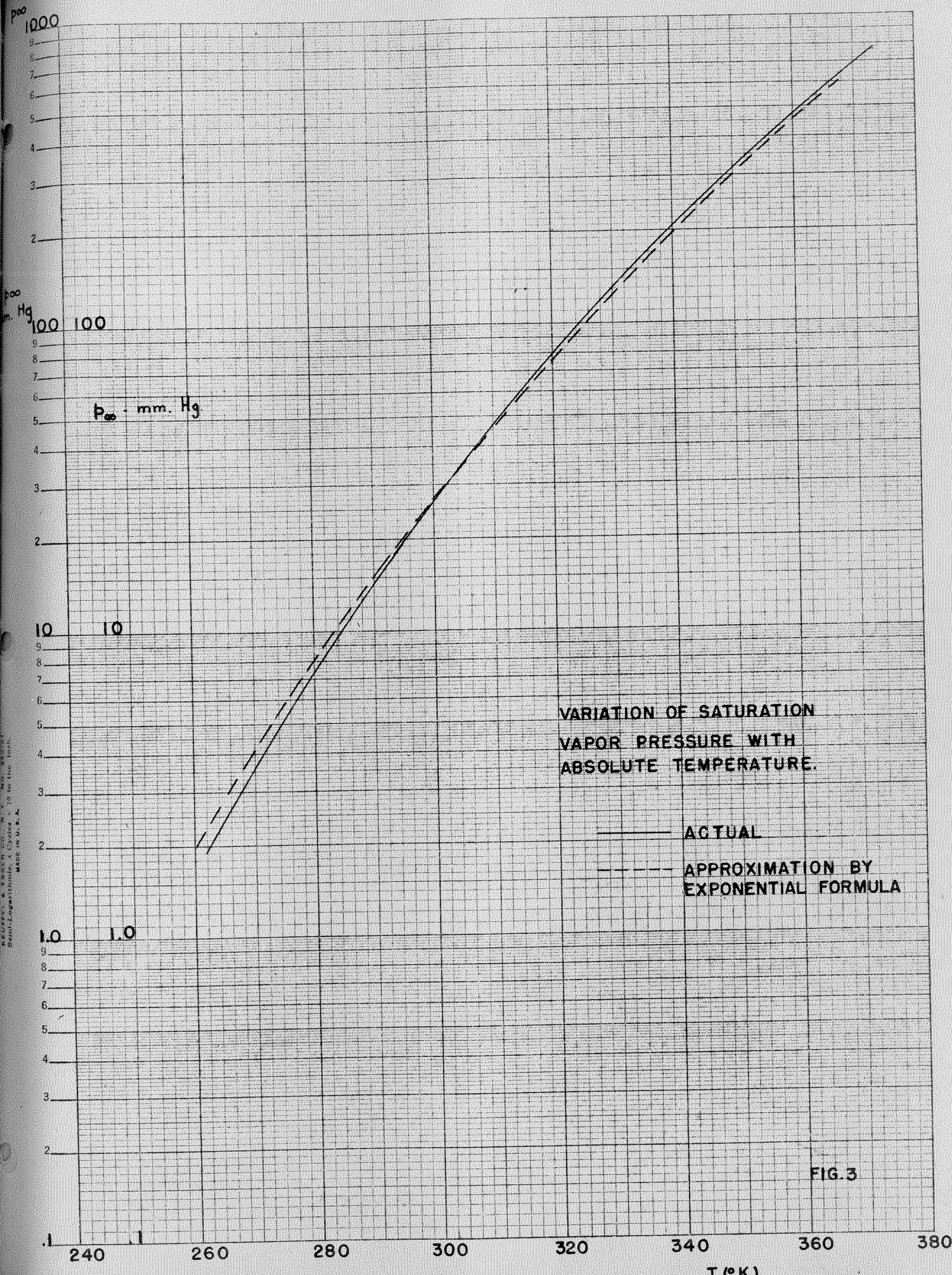
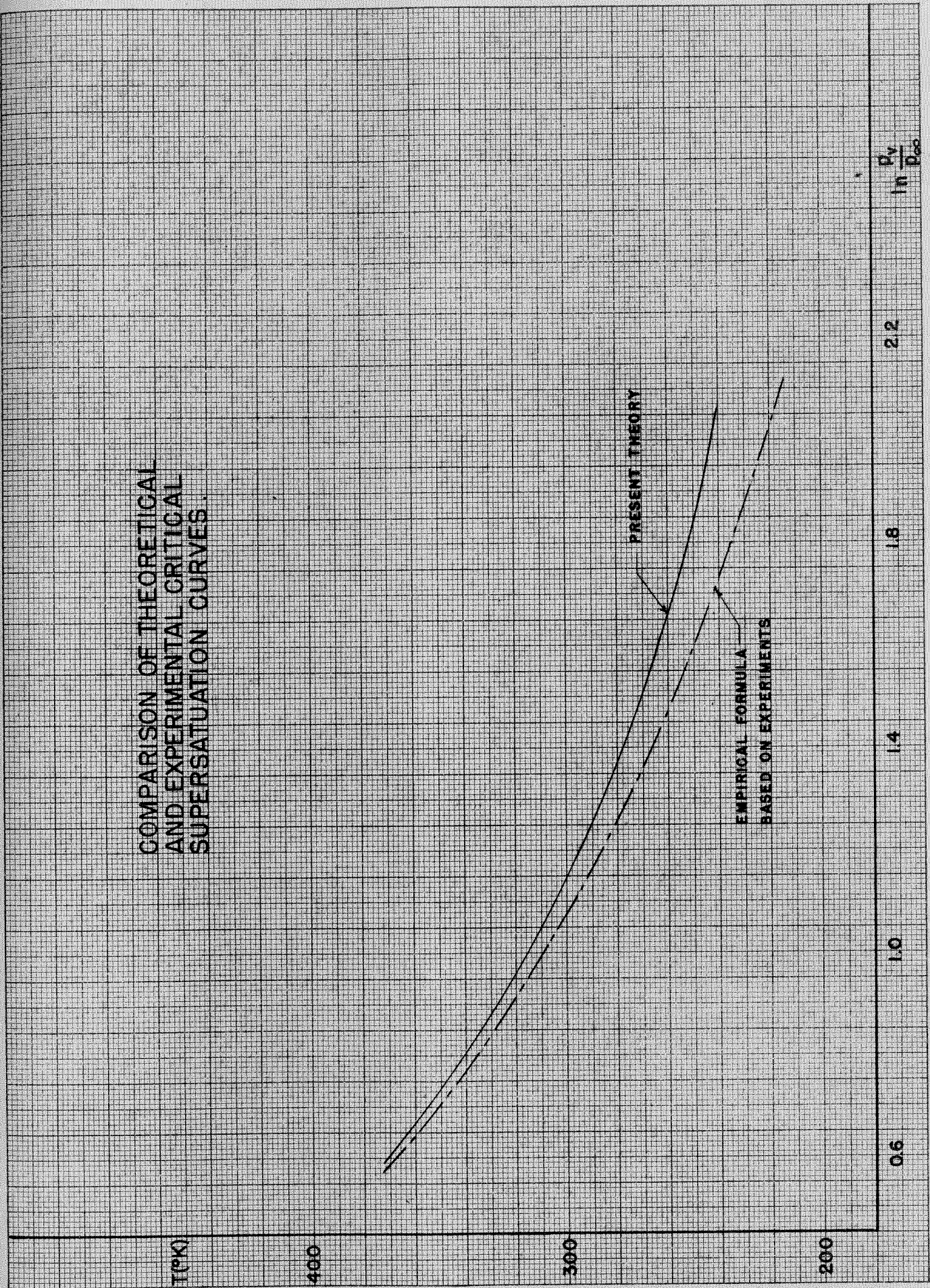


FIG. 3

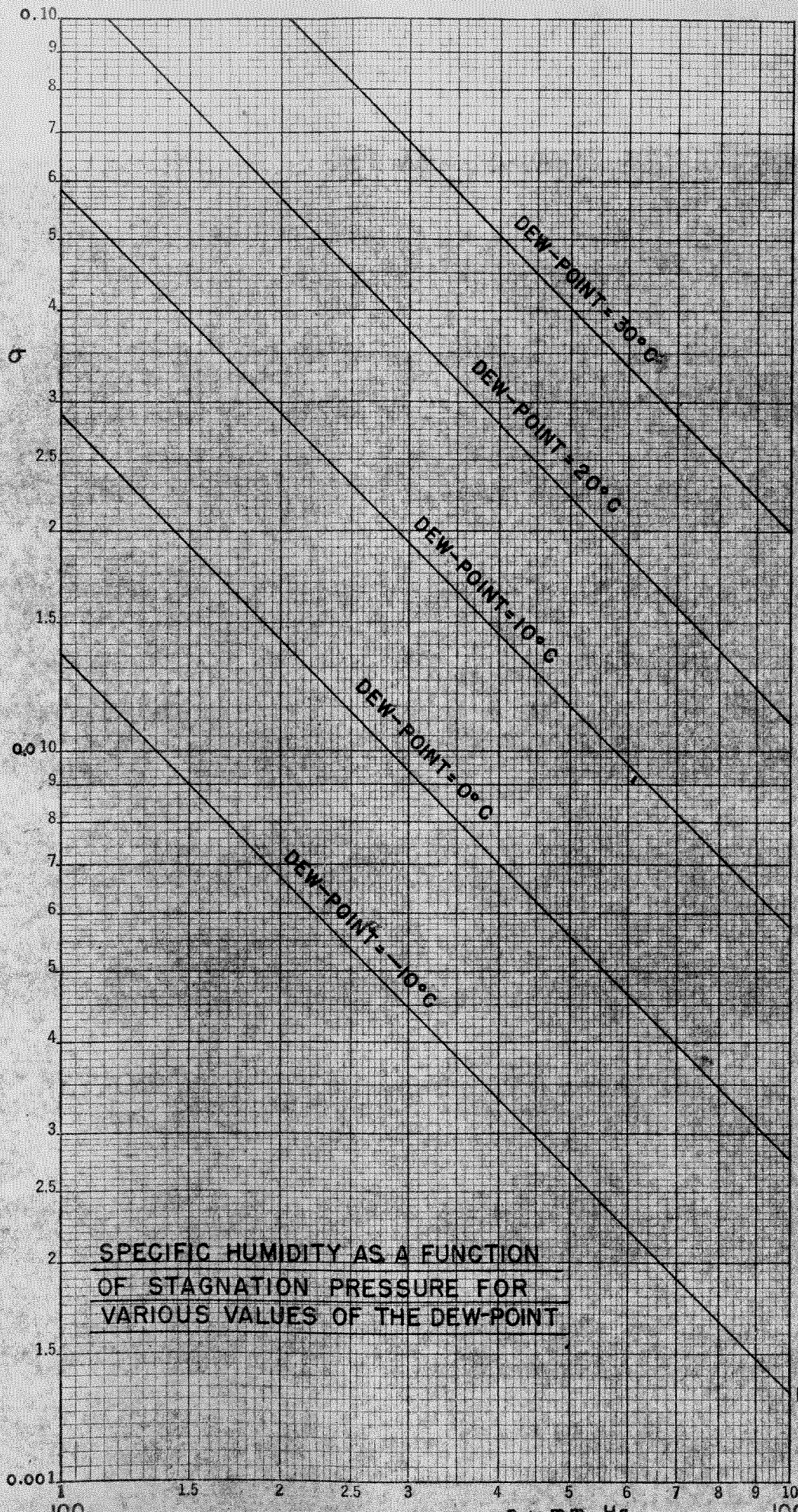
CHARLES & JOSEPH GLENN, INC. NEW YORK  
 SEMI-CONDUCTOR DIVISION, 100 W. 40th ST. N.Y.C. 18, N.Y.  
 MADE IN U.S.A.



COMPARISON OF THEORETICAL  
AND EXPERIMENTAL CRITICAL  
SUPERSATURATION CURVES



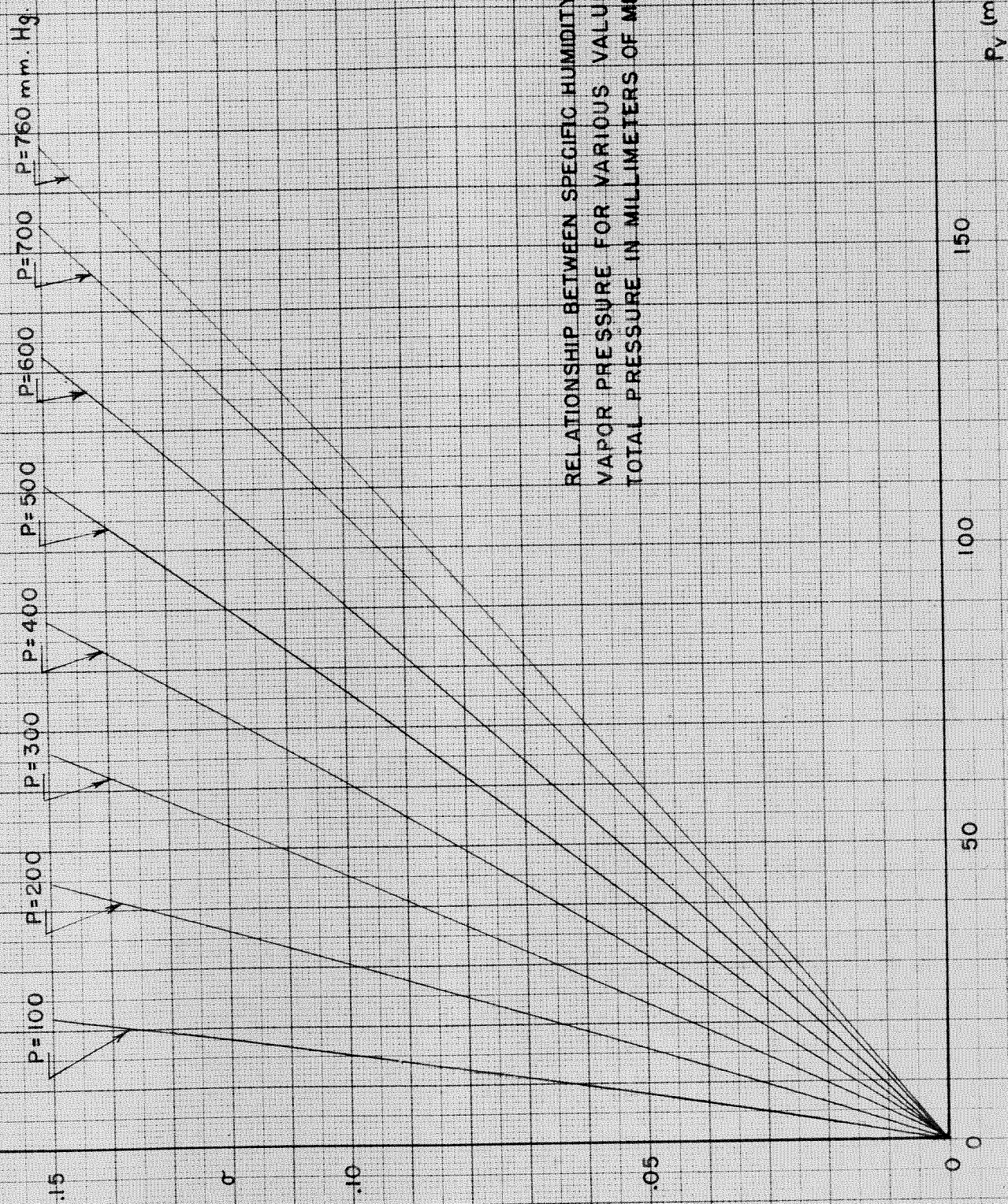




SPECIFIC HUMIDITY AS A FUNCTION  
OF STAGNATION PRESSURE FOR  
VARIOUS VALUES OF THE DEW-POINT

FIG. 5

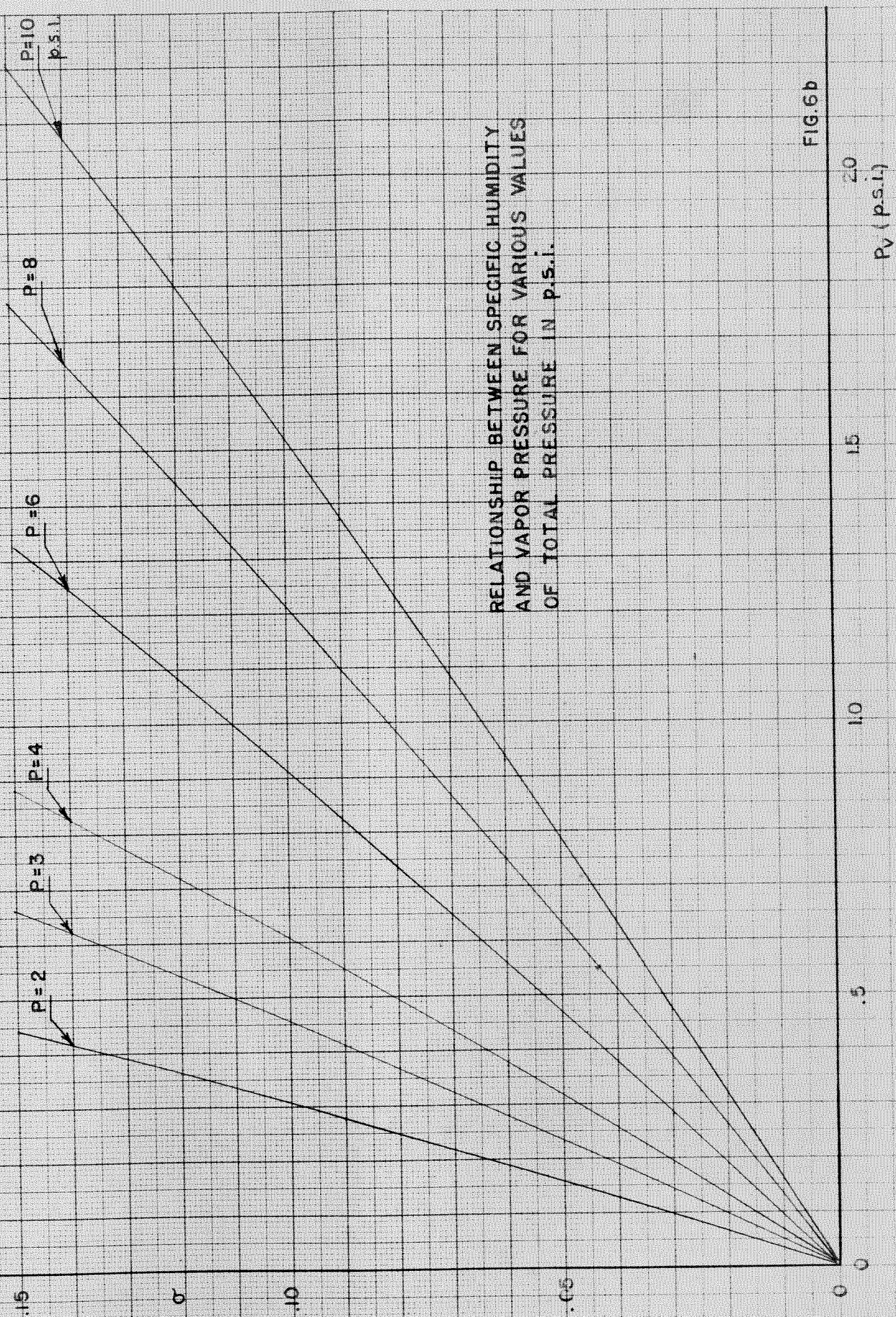




RELATIONSHIP BETWEEN SPECIFIC HUMIDITY AND  
VAPOR PRESSURE FOR VARIOUS VALUES OF  
TOTAL PRESSURE IN MILLIMETERS OF MERCURY

FIG. 6 a





RELATIONSHIP BETWEEN SPECIFIC HUMIDITY  
AND VAPOR PRESSURE FOR VARIOUS VALUES  
OF TOTAL PRESSURE IN p.s.i.

FIG. 6b

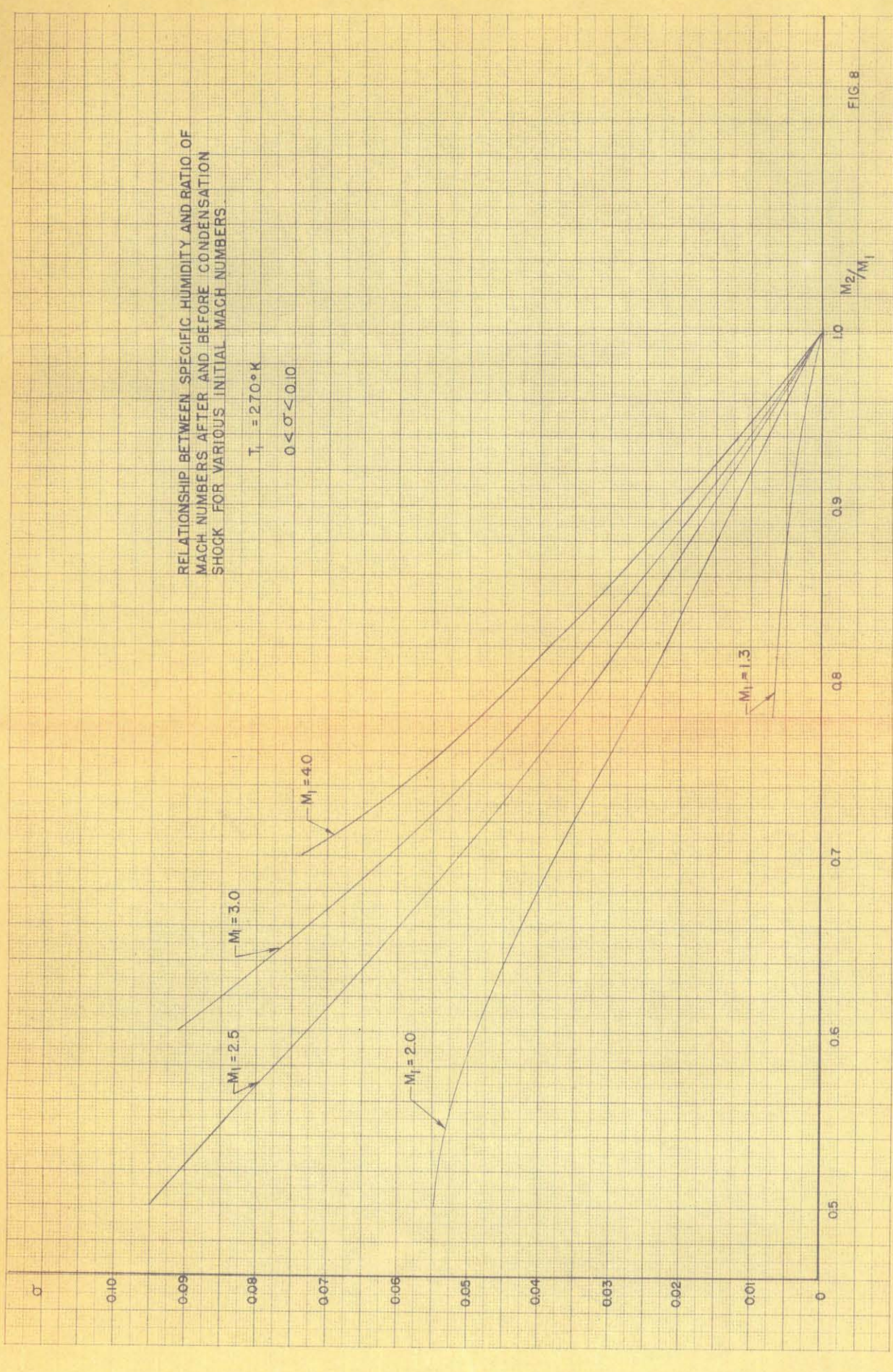






RELATIONSHIP BETWEEN SPECIFIC HUMIDITY AND RATIO OF  
MACH NUMBERS AFTER AND BEFORE CONDENSATION  
SHOCK FOR VARIOUS INITIAL MACH NUMBERS

$T_1 = 270^\circ\text{K}$   
 $0 < \sigma < 0.10$





RELATIONSHIP BETWEEN SPECIFIC HUMIDITY AND RATIO OF MACH NUMBERS AFTER AND BEFORE CONDENSATION SHOCK FOR VARIOUS INITIAL MACH NUMBERS.

$T_1 = 300^\circ\text{K}$   
 $0 < \sigma < 0.10$

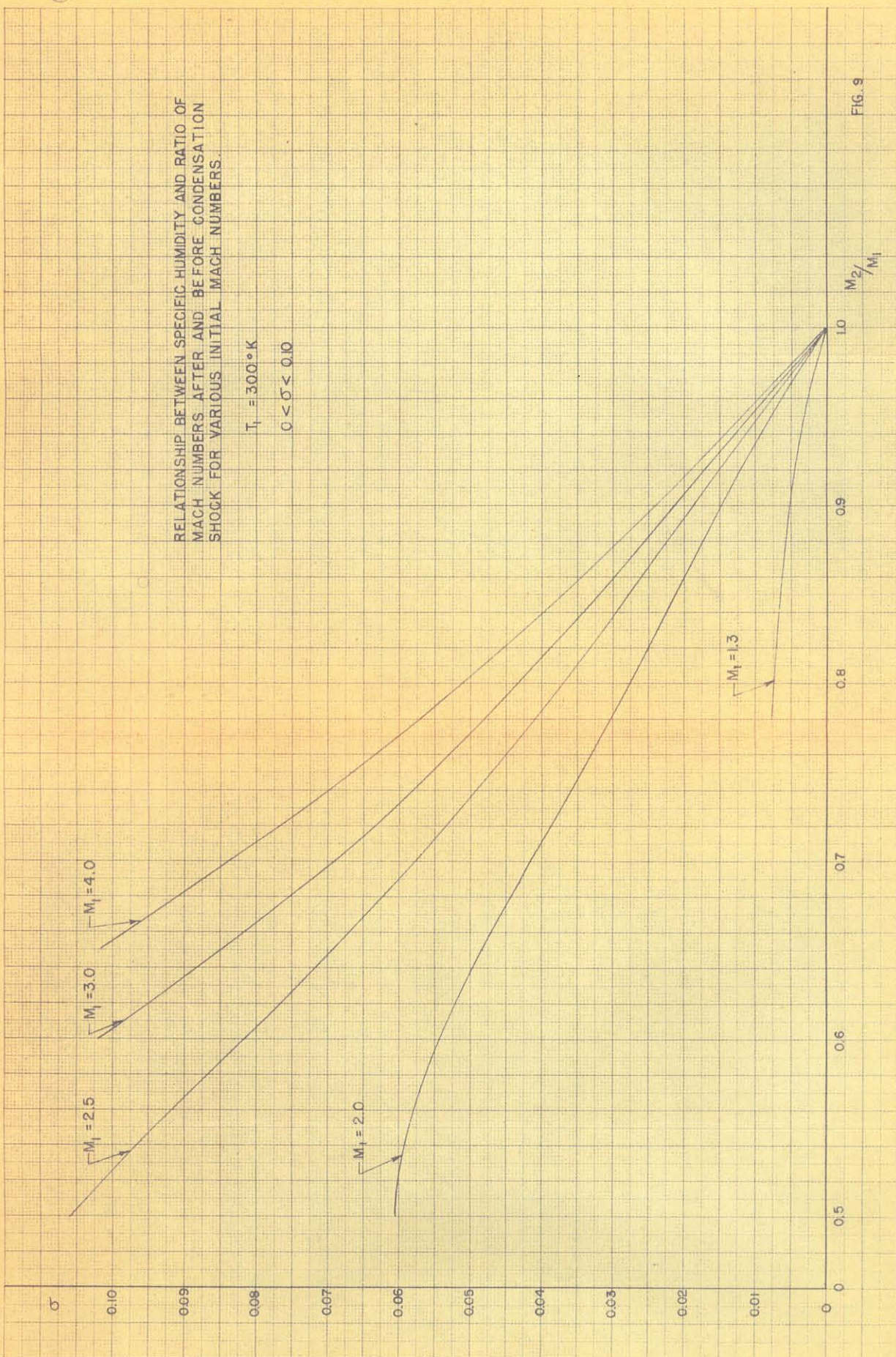


FIG. 9



RELATIONSHIP BETWEEN SPECIFIC HUMIDITY AND RATIO OF  
MACH NUMBERS AFTER AND BEFORE CONDENSATION  
SHOCK FOR VARIOUS INITIAL MACH NUMBERS

$T_1 = 320^\circ\text{K}$   
 $0 < \sigma < 0.10$

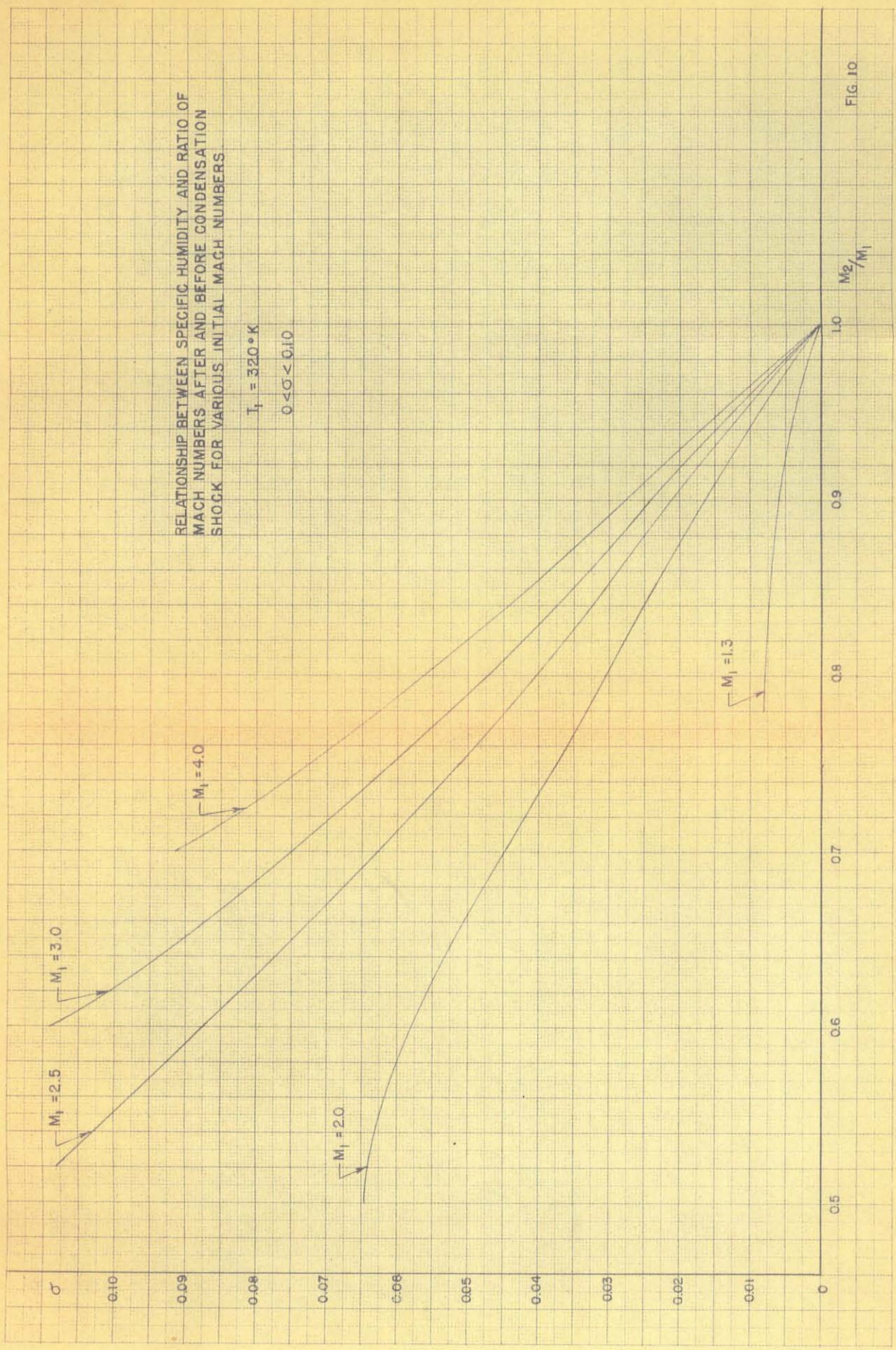


FIG. 10





RELATIONSHIP BETWEEN SPECIFIC HUMIDITY AND RATIO OF  
MACH NUMBERS AFTER AND BEFORE CONDENSATION  
SHOCK FOR VARIOUS INITIAL MACH NUMBERS.

$T_1 = 3550^\circ \text{K}$   
 $0 < \sigma < 0.10$

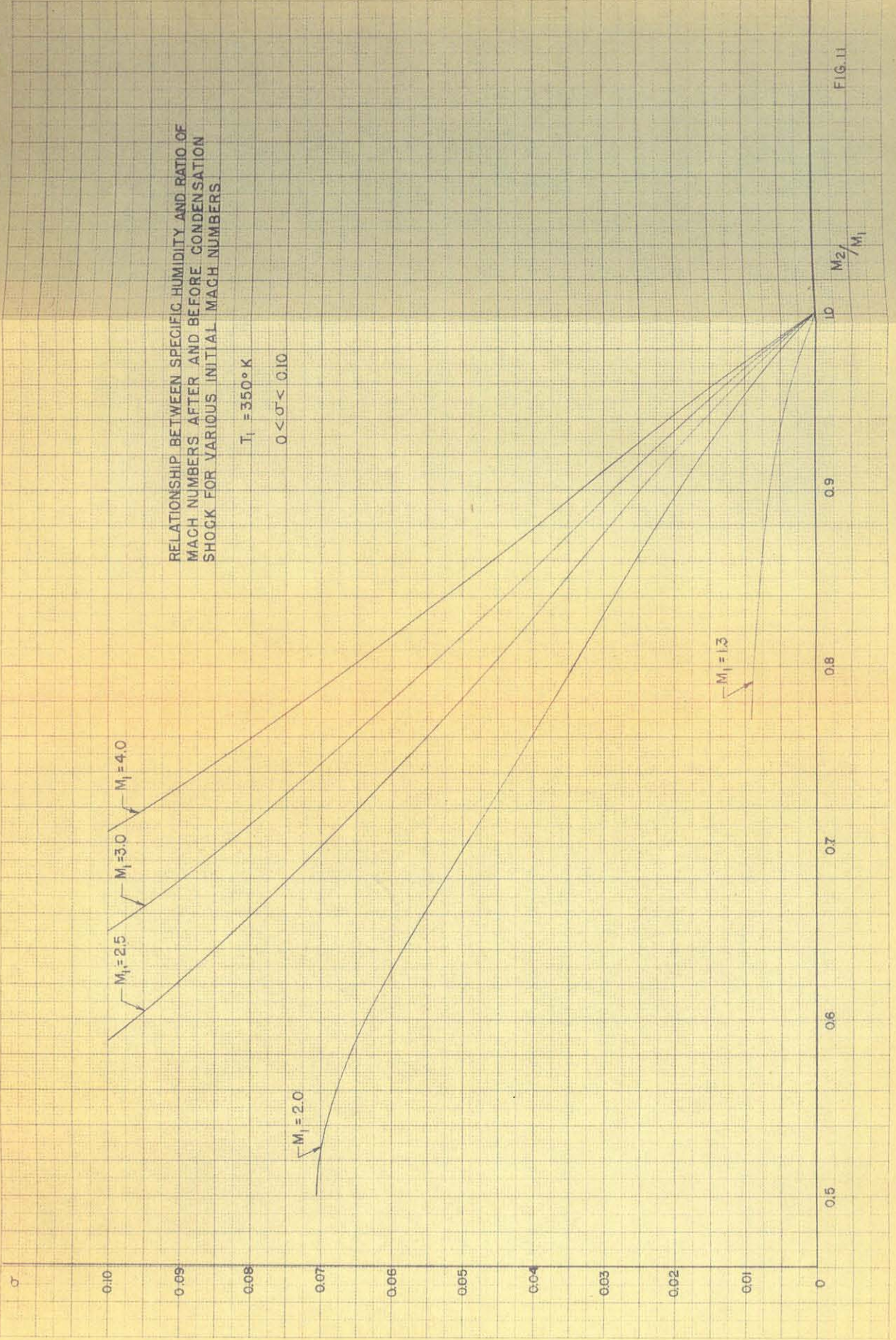
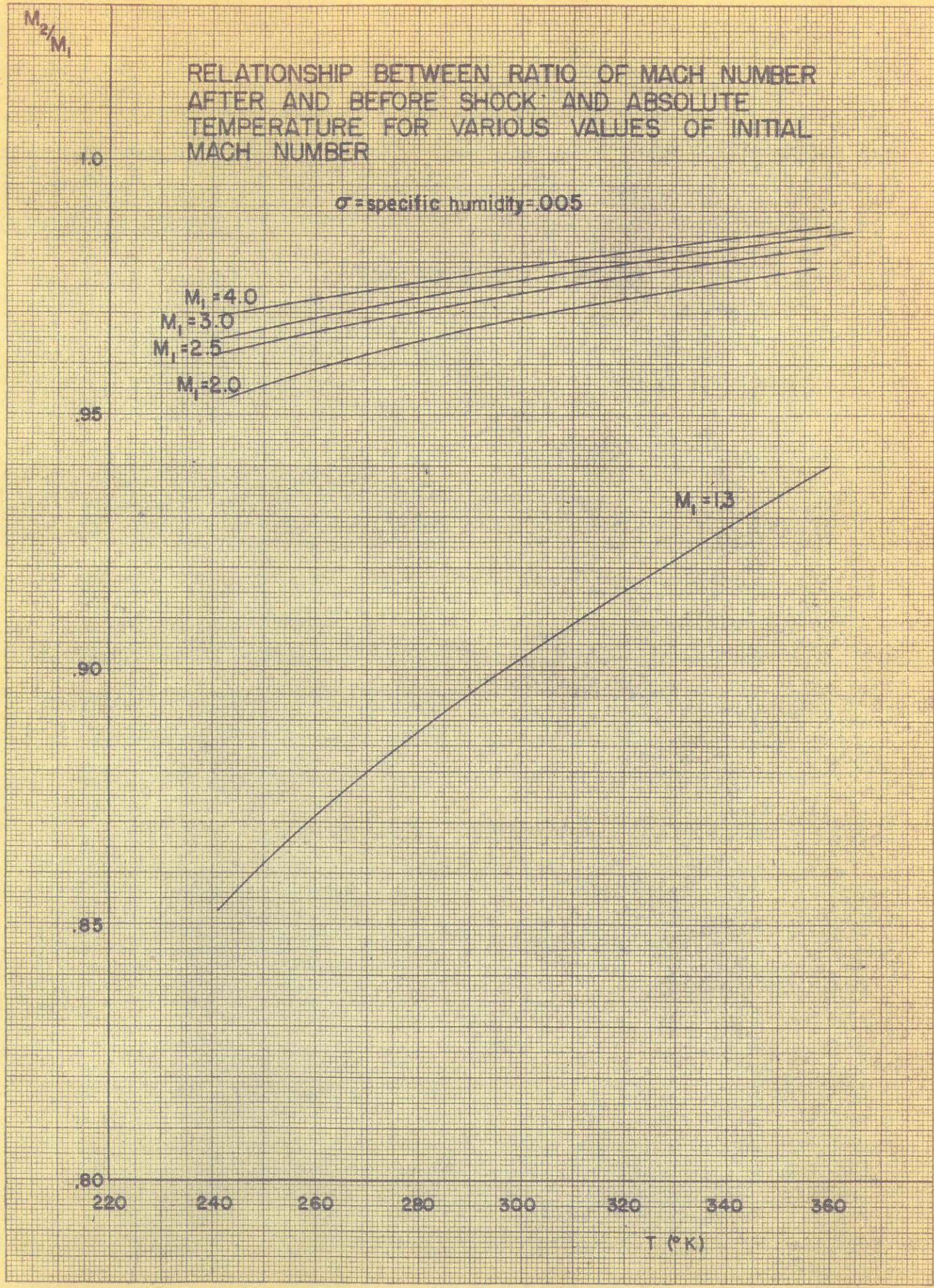
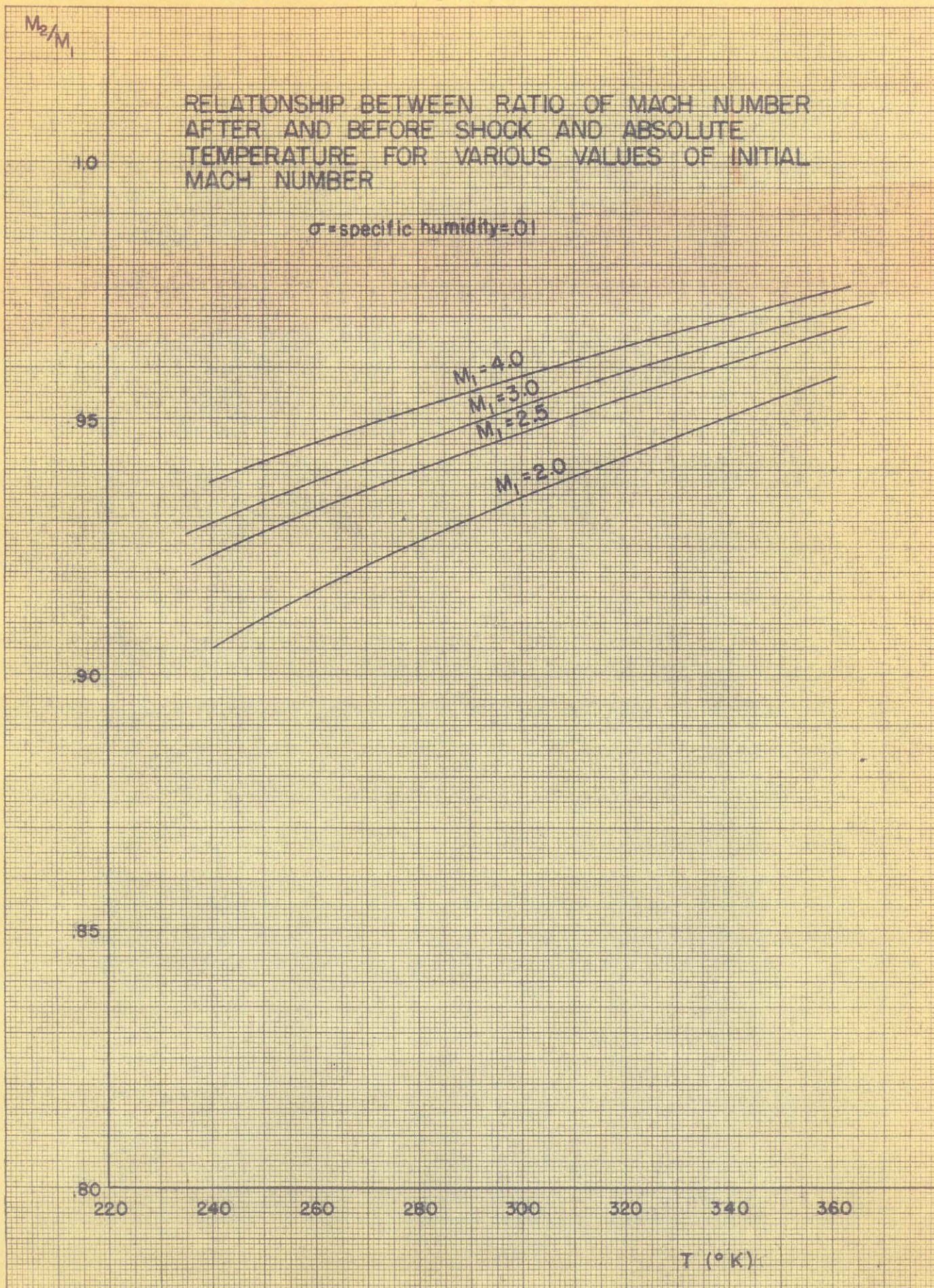


FIG. 11

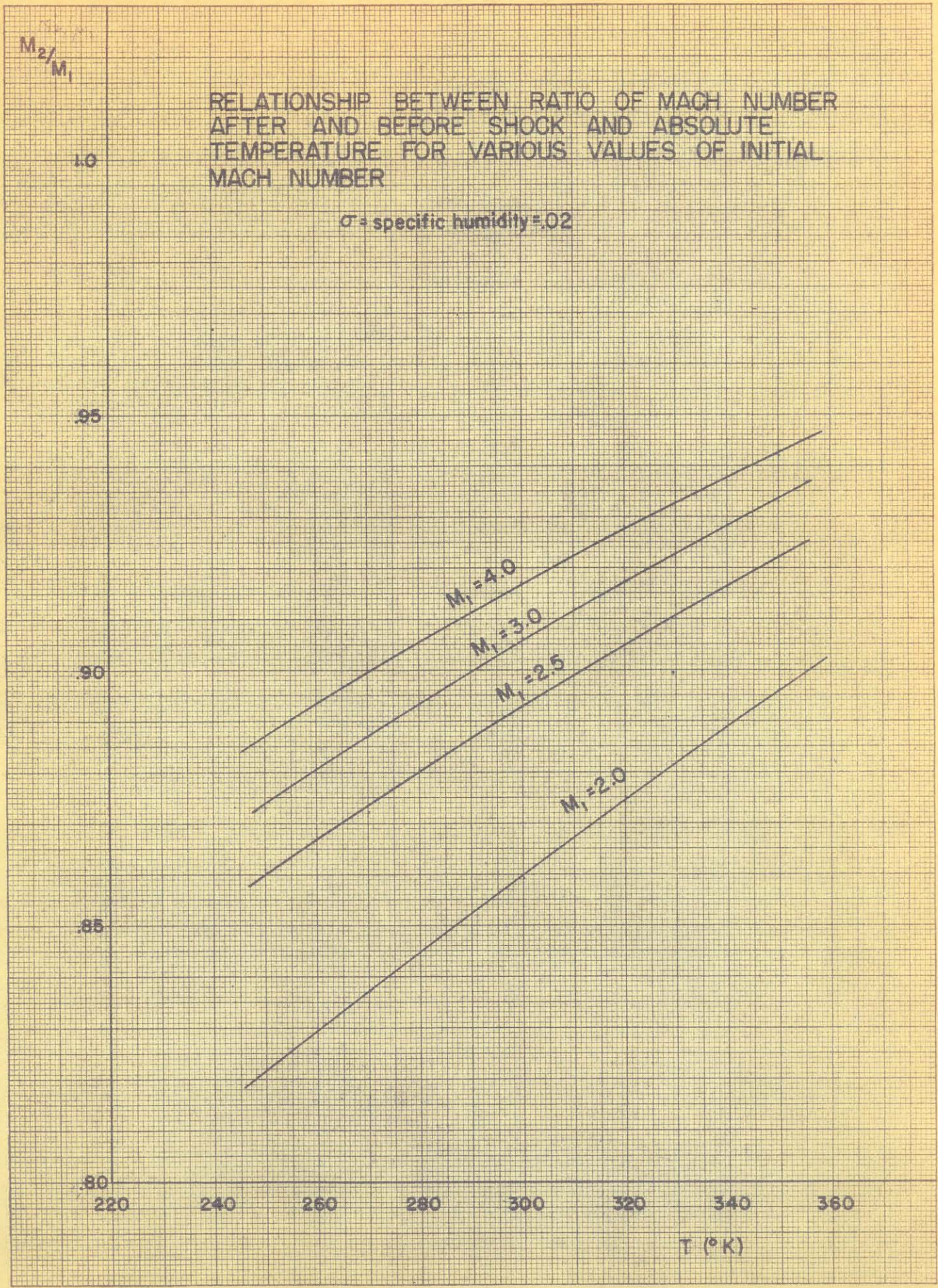














$M_2/M_1$

RELATIONSHIP BETWEEN RATIO OF MACH NUMBER  
AFTER AND BEFORE SHOCK AND ABSOLUTE  
TEMPERATURE FOR VARIOUS VALUES OF INITIAL  
MACH NUMBER

$\sigma$  = specific humidity = 0.4

1.0

.90

.80

.70

.60

220

240

260

280

300

320

340

360

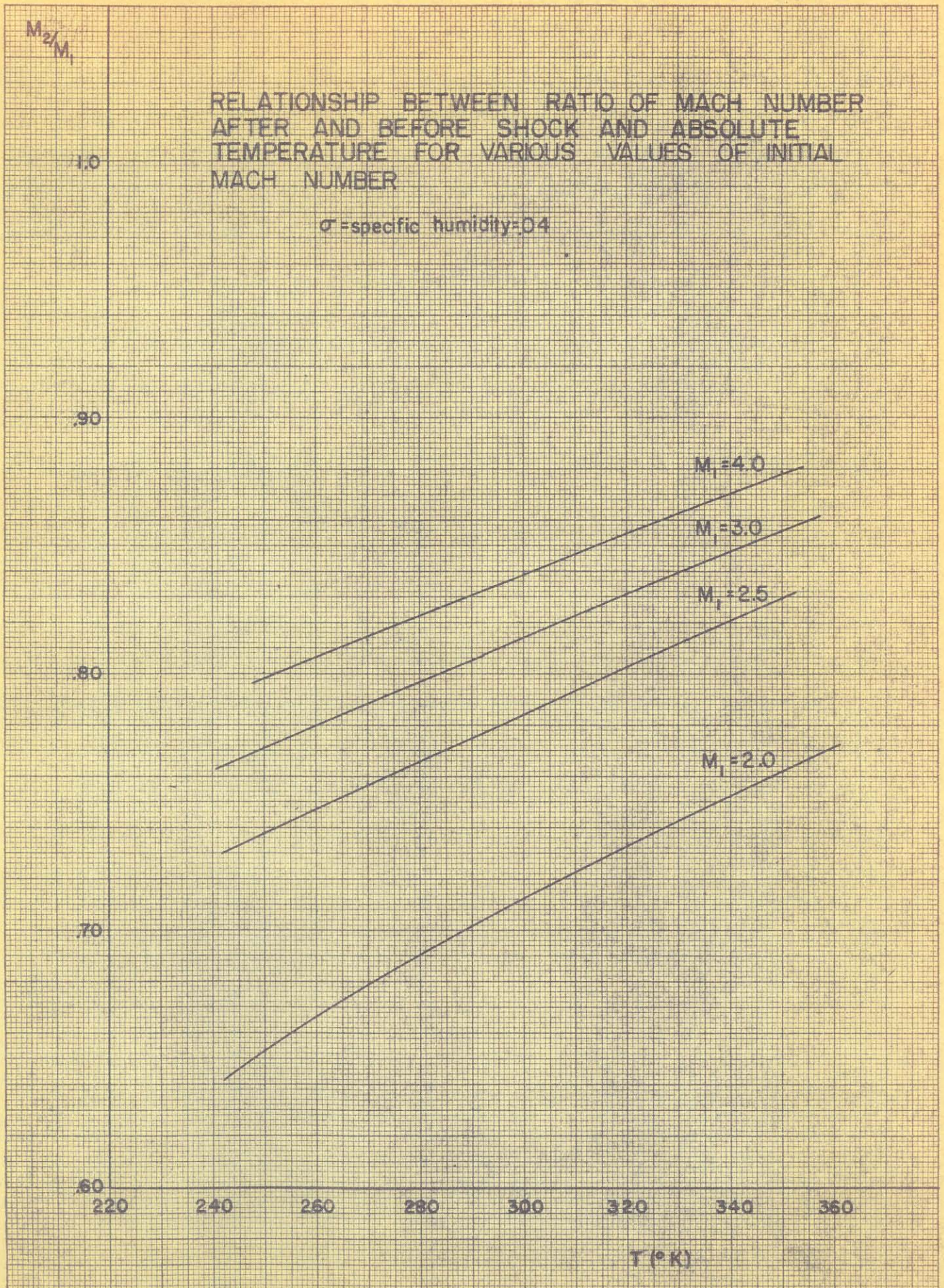
$T$  ( $^{\circ}$ K)

$M_1 = 4.0$

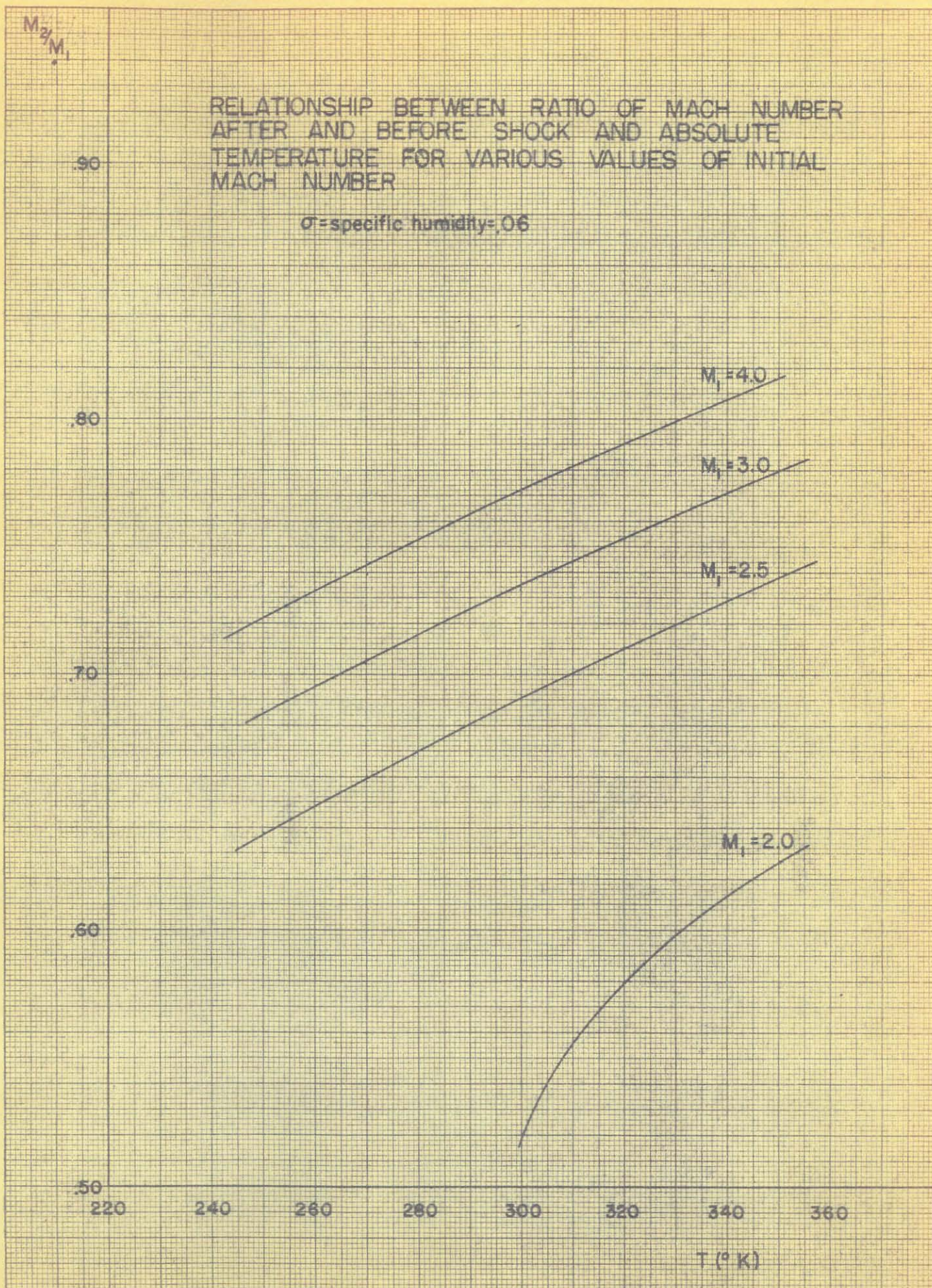
$M_1 = 3.0$

$M_1 = 2.5$

$M_1 = 2.0$









$M_2/M_1$

RELATIONSHIP BETWEEN RATIO OF MACH NUMBER  
AFTER AND BEFORE SHOCK AND ABSOLUTE  
TEMPERATURE FOR VARIOUS VALUES OF INITIAL  
MACH NUMBER

$\sigma$  = specific humidity = .08

.90

.80

.70

.60

.50

220

240

260

280

300

320

340

360

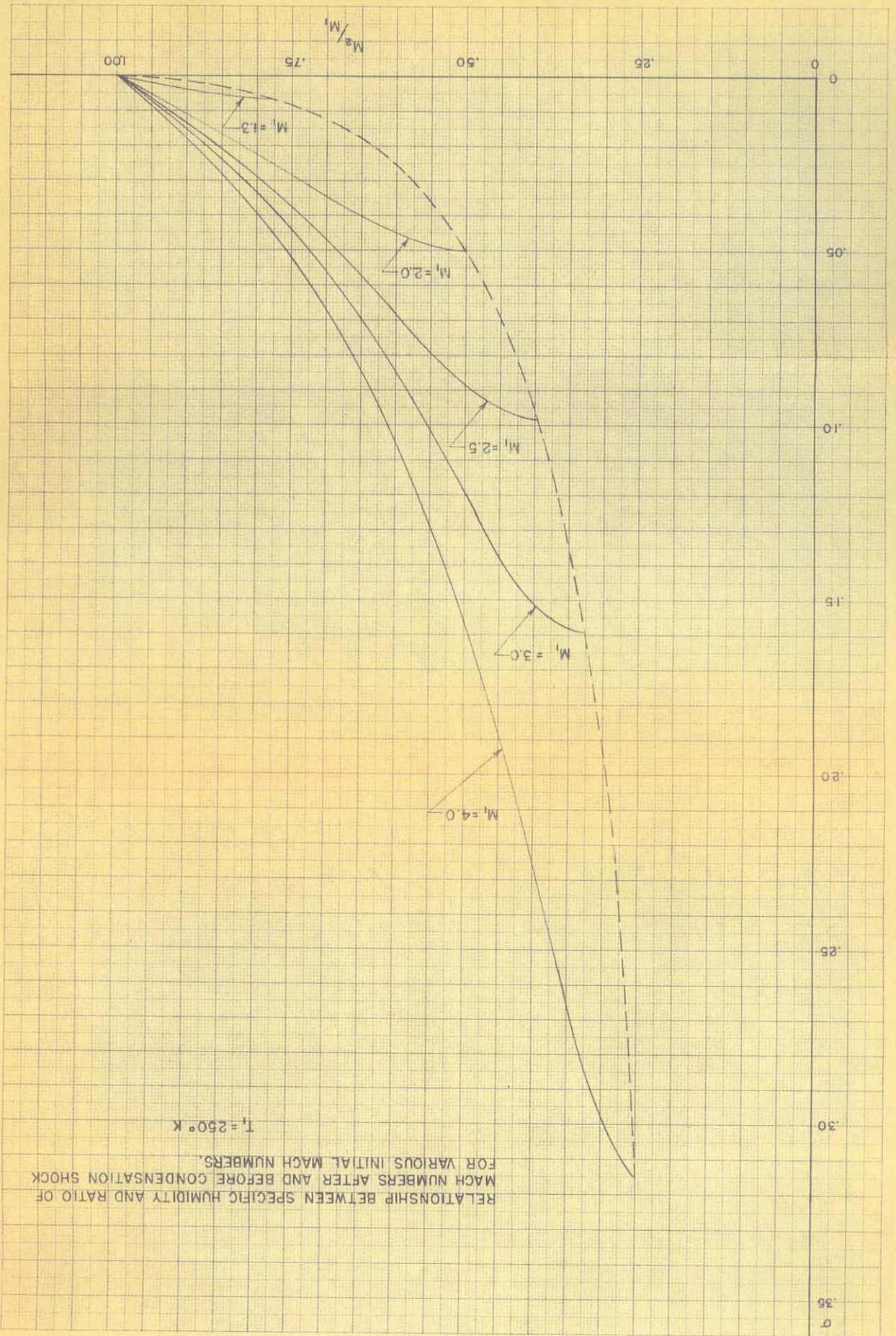
T (°K)

$M_1 = 4.0$

$M_1 = 3.0$

$M_1 = 2.5$







RELATIONSHIP BETWEEN SPECIFIC HUMIDITY AND RATIO OF  
MACH NUMBERS AFTER AND BEFORE CONDENSATION  
SHOCK FOR VARIOUS INITIAL MACH NUMBERS  
INITIAL TEMPERATURE,  $T_1 = 270^\circ\text{K}$

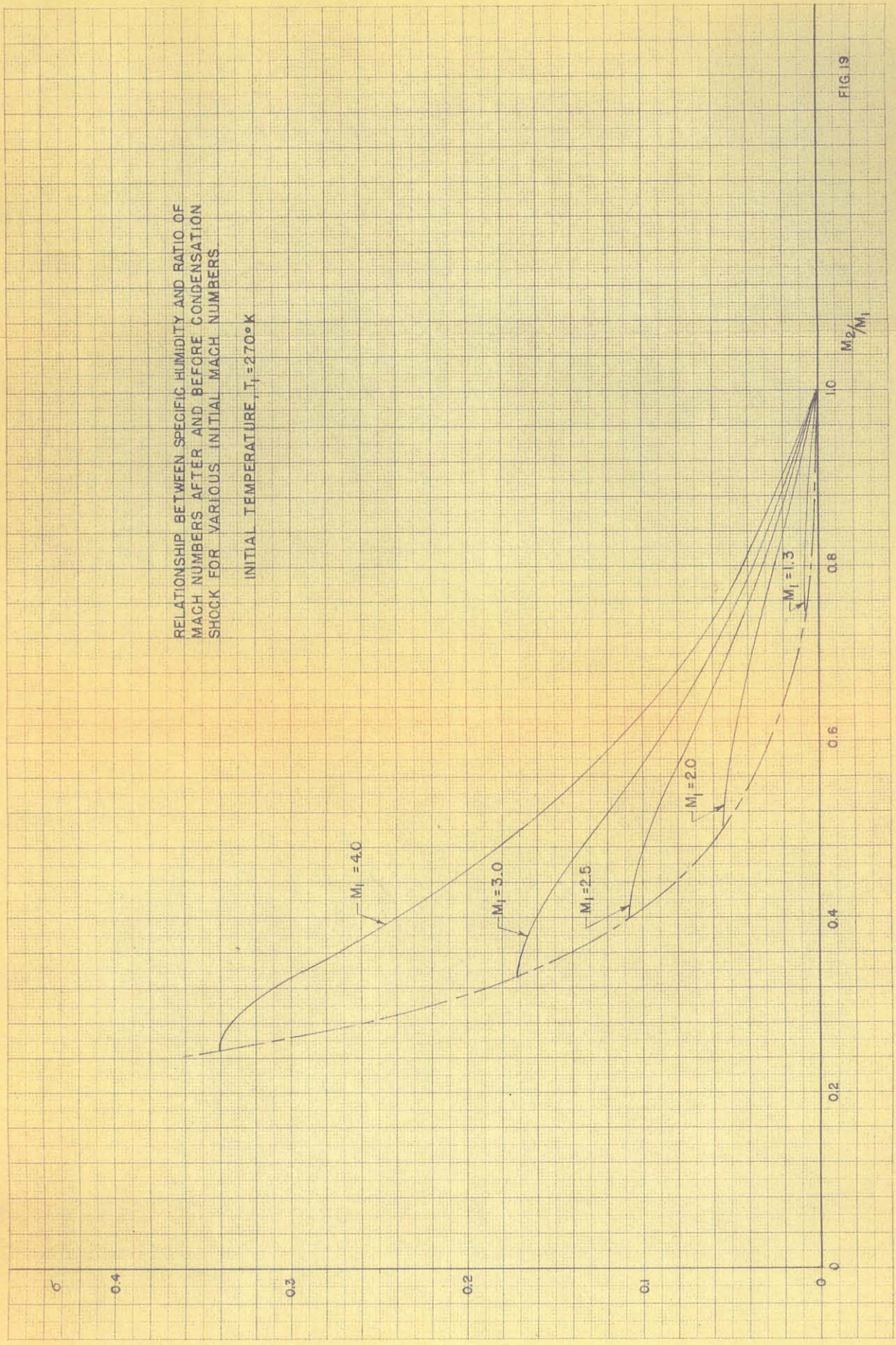


FIG. 19





RELATIONSHIP BETWEEN SPECIFIC HUMIDITY AND RATIO OF  
MACH NUMBERS AFTER AND BEFORE CONDENSATION  
SHOCK FOR VARIOUS INITIAL MACH NUMBERS.

INITIAL TEMPERATURE,  $T_1 = 300^\circ\text{K}$

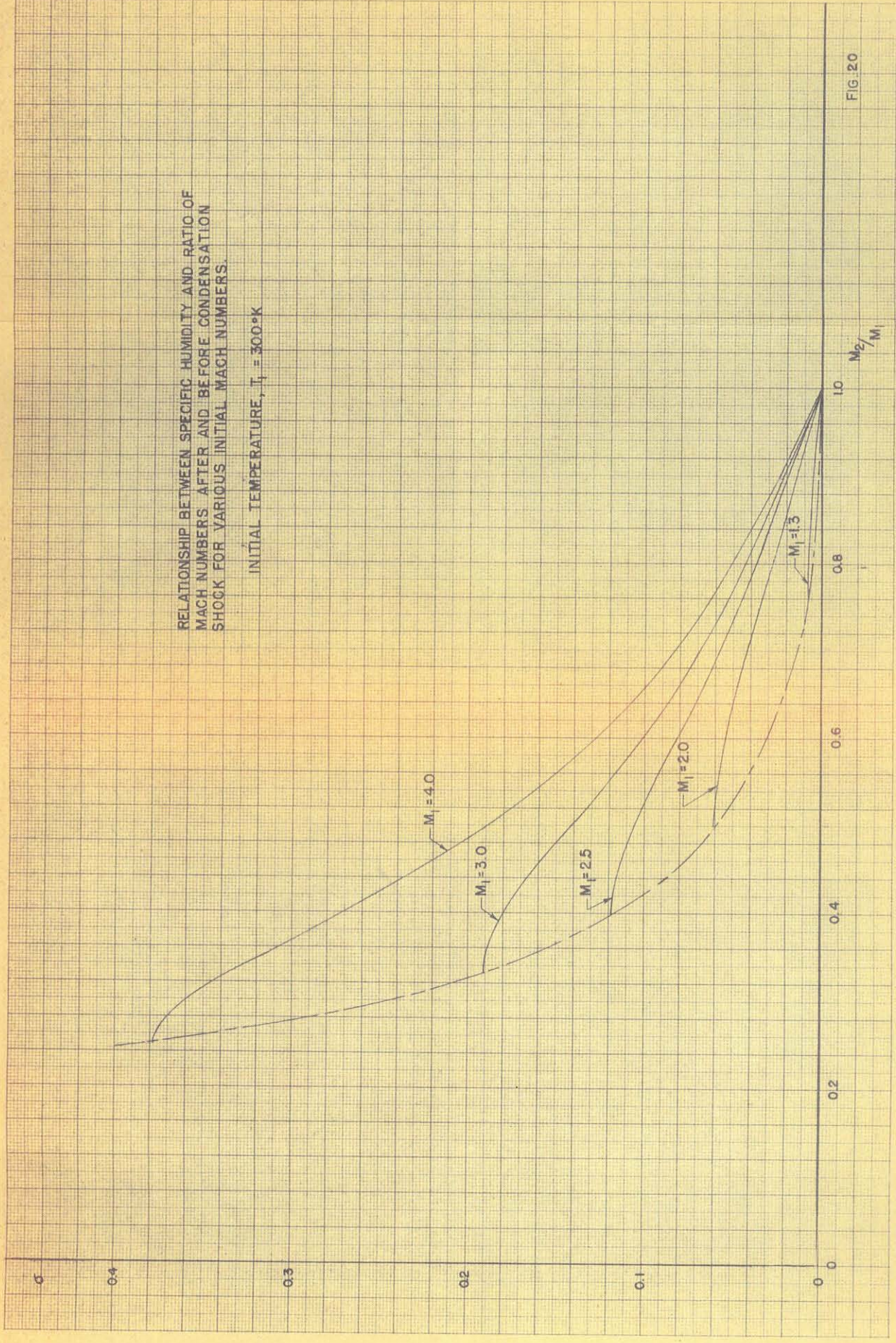


FIG. 20





RELATIONSHIP BETWEEN SPECIFIC HUMIDITY AND RATIO OF  
MACH NUMBERS AFTER AND BEFORE CONDENSATION  
SHOCK FOR VARIOUS INITIAL MACH NUMBERS

INITIAL TEMPERATURE,  $T_1 = 320^\circ\text{K}$

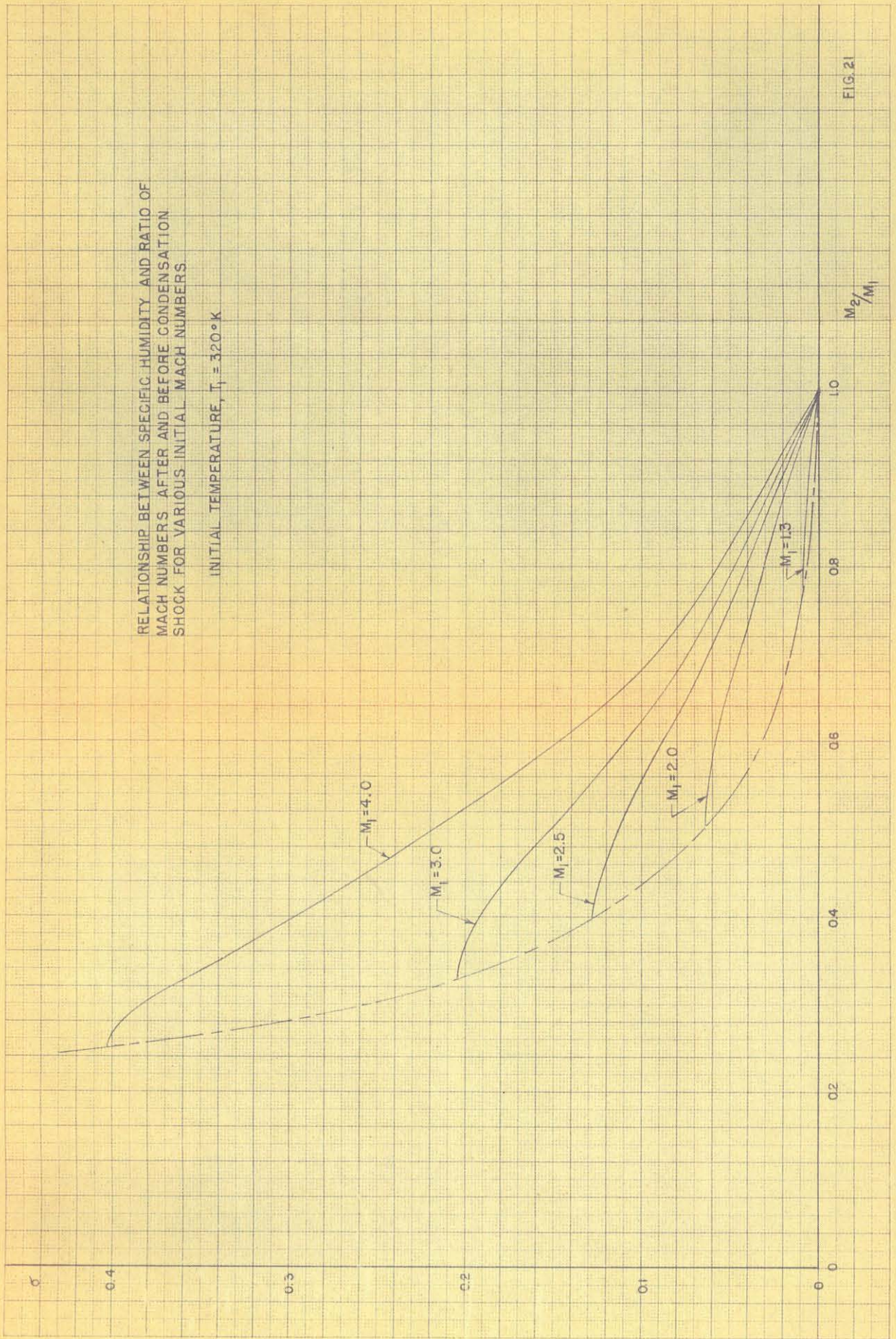


FIG. 21



RELATIONSHIP BETWEEN SPECIFIC HUMIDITY AND RATIO OF  
MACH NUMBERS AFTER AND BEFORE CONDENSATION  
SHOCK FOR VARIOUS INITIAL MACH NUMBERS.

INITIAL TEMPERATURE,  $T_1 = 350^\circ\text{K}$

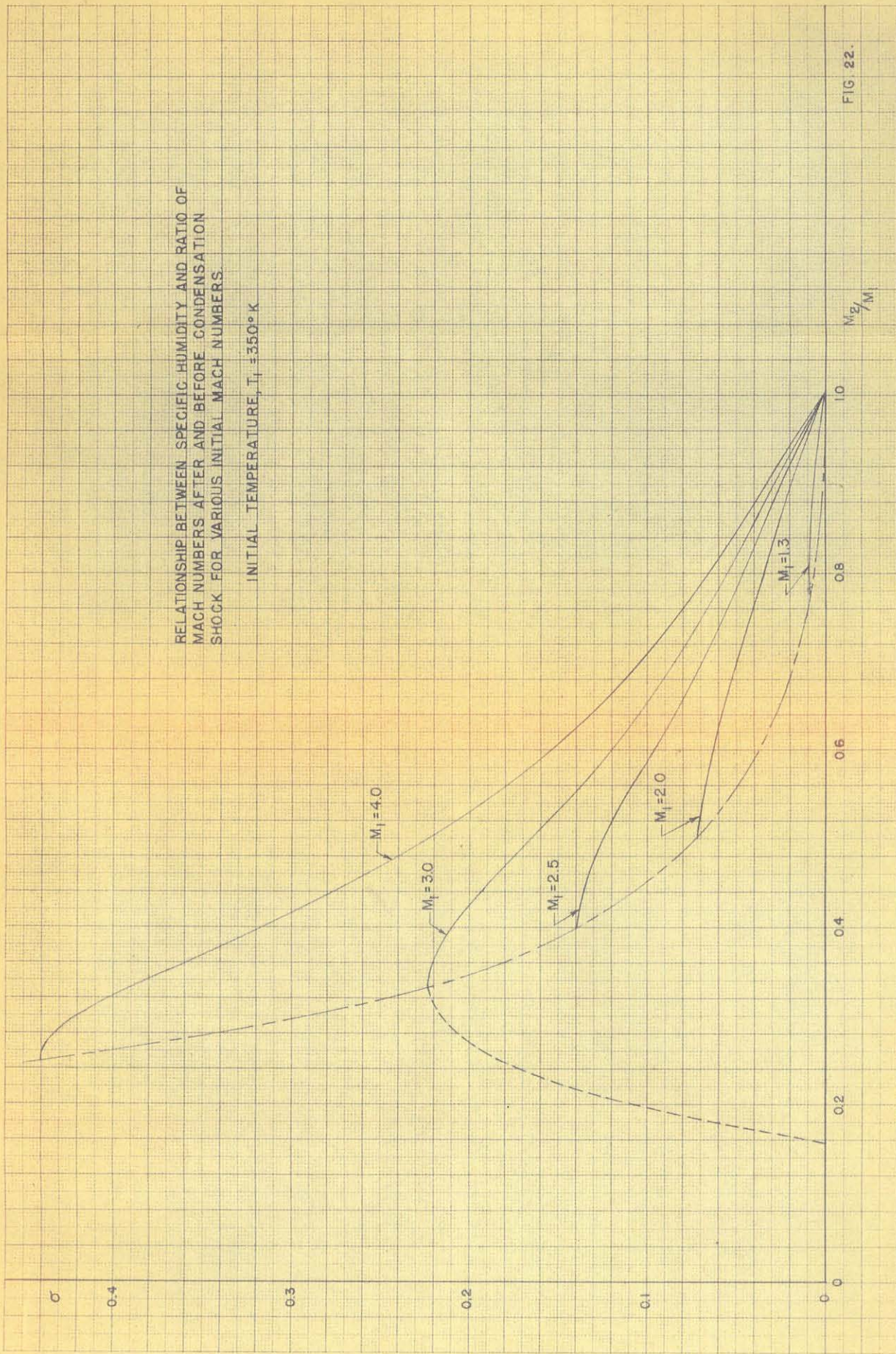


FIG. 22.



RELATIONSHIP BETWEEN RATIO OF PRESSURES  
AND RATIO OF MACH NUMBERS AFTER AND BEFORE  
SHOCK FOR VARIOUS INITIAL MACH NUMBERS.

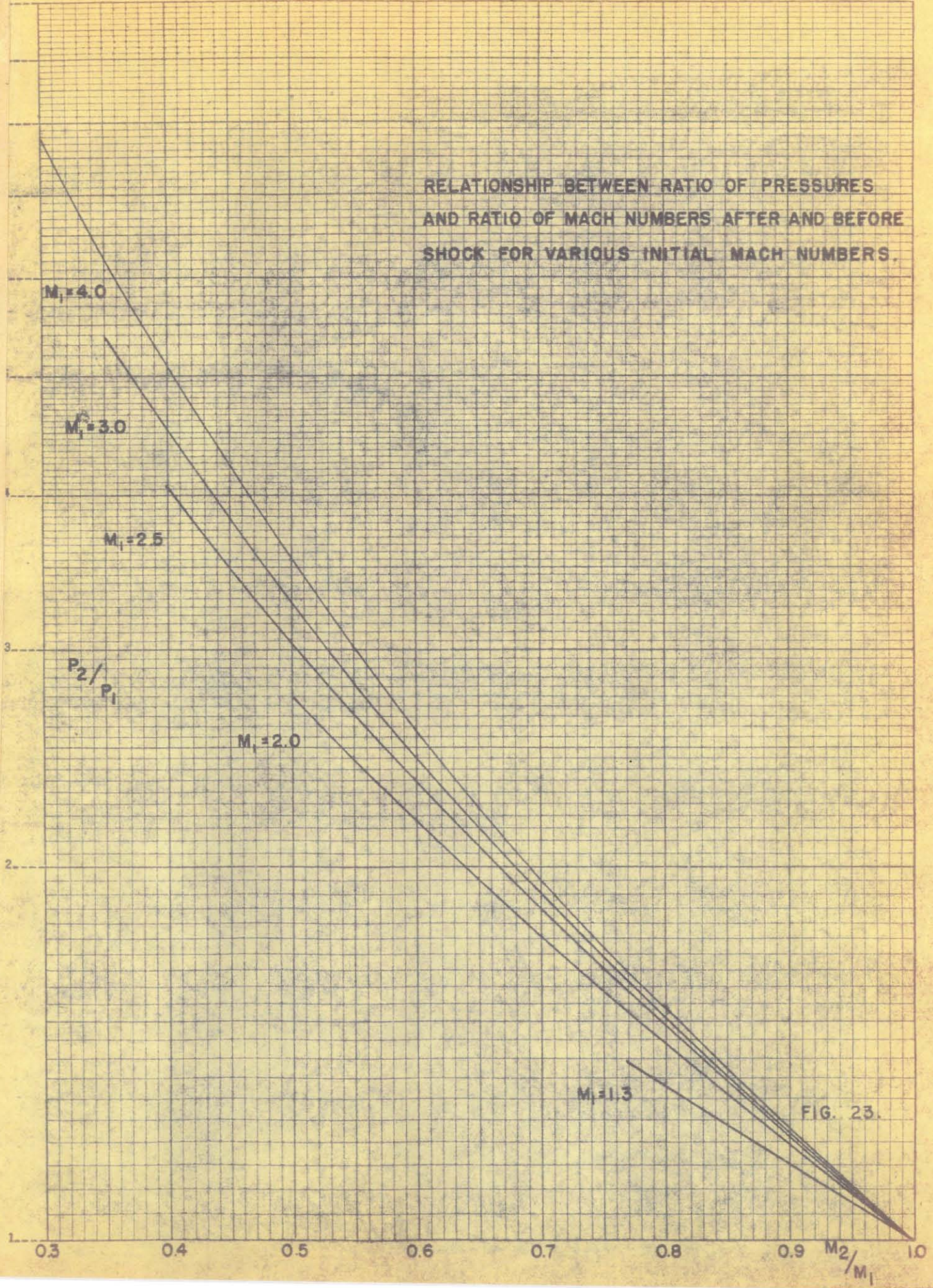
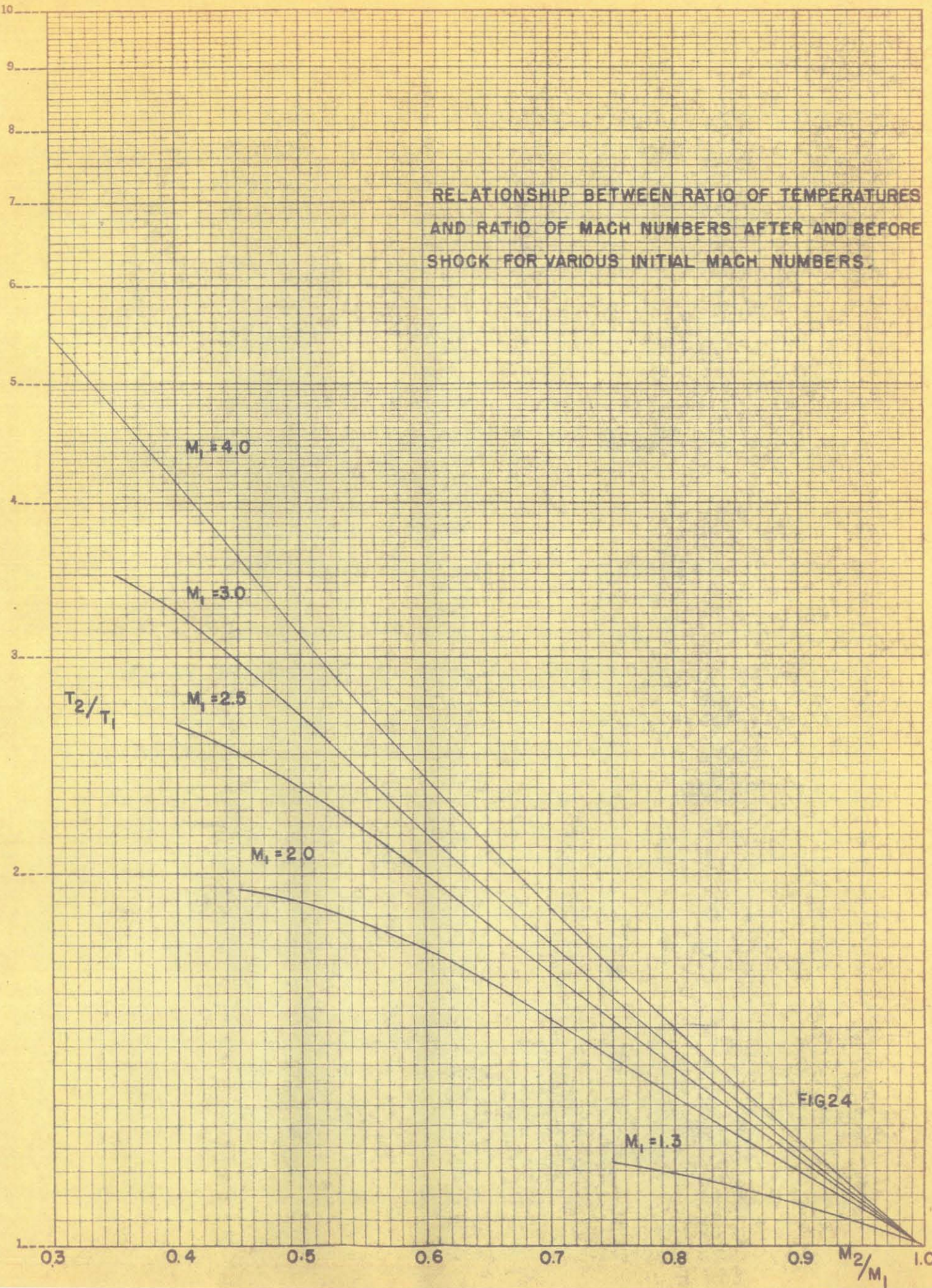


FIG. 23.



RELATIONSHIP BETWEEN RATIO OF TEMPERATURES AND RATIO OF MACH NUMBERS AFTER AND BEFORE SHOCK FOR VARIOUS INITIAL MACH NUMBERS.



MADE IN U.S.A.

FIG24



RELATION BETWEEN TEMPERATURE, PRESSURE, MACH NUMBER  
AND AREA RATIO FOR SECTIONS DOWNSTREAM OF THROAT

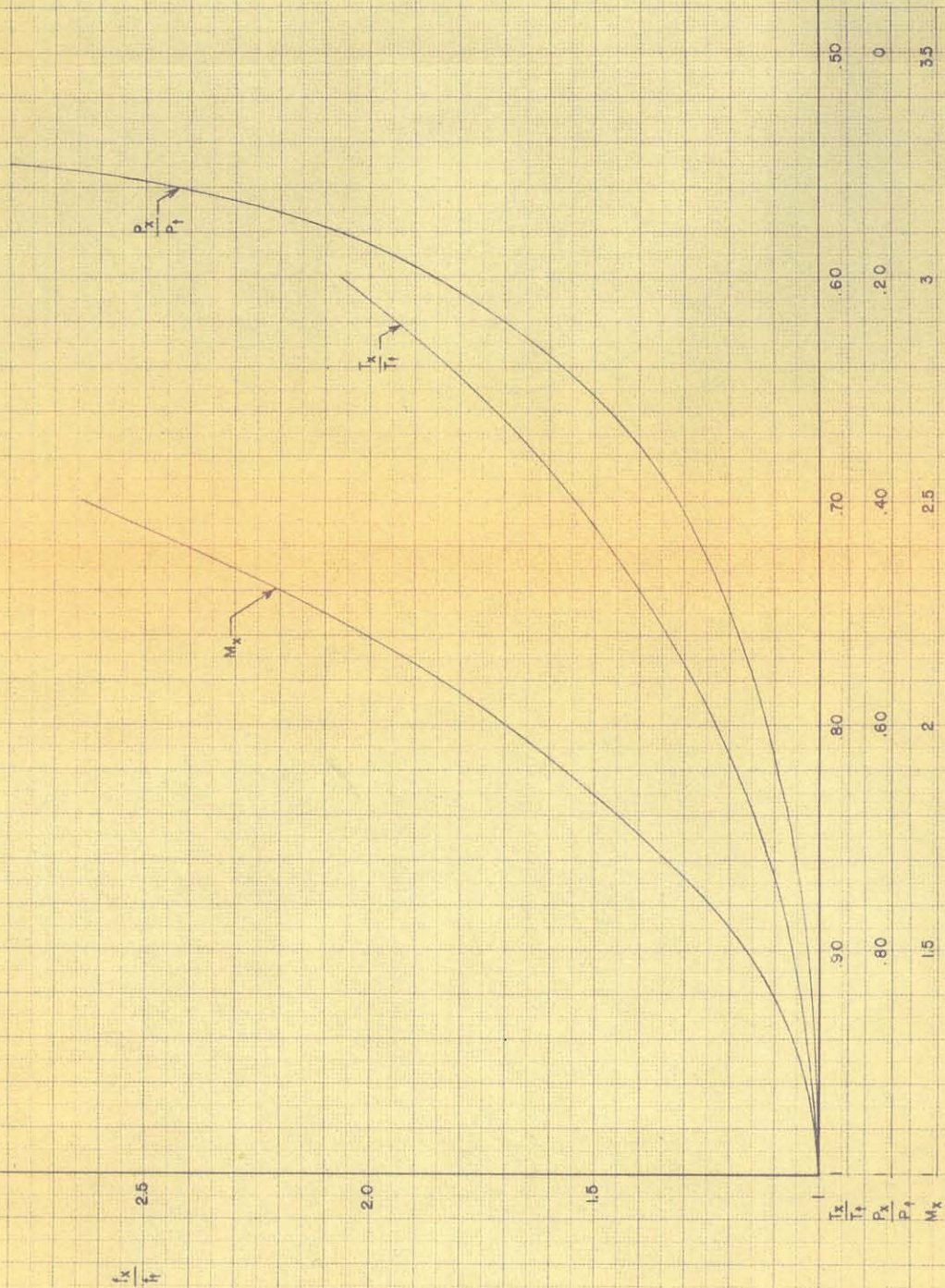


FIG. 25



DETERMINATION OF CONDITIONS  
FOR COLLAPSE OF SUPERSATURATED  
STATE IN ILLUSTRATIVE EXAMPLE.

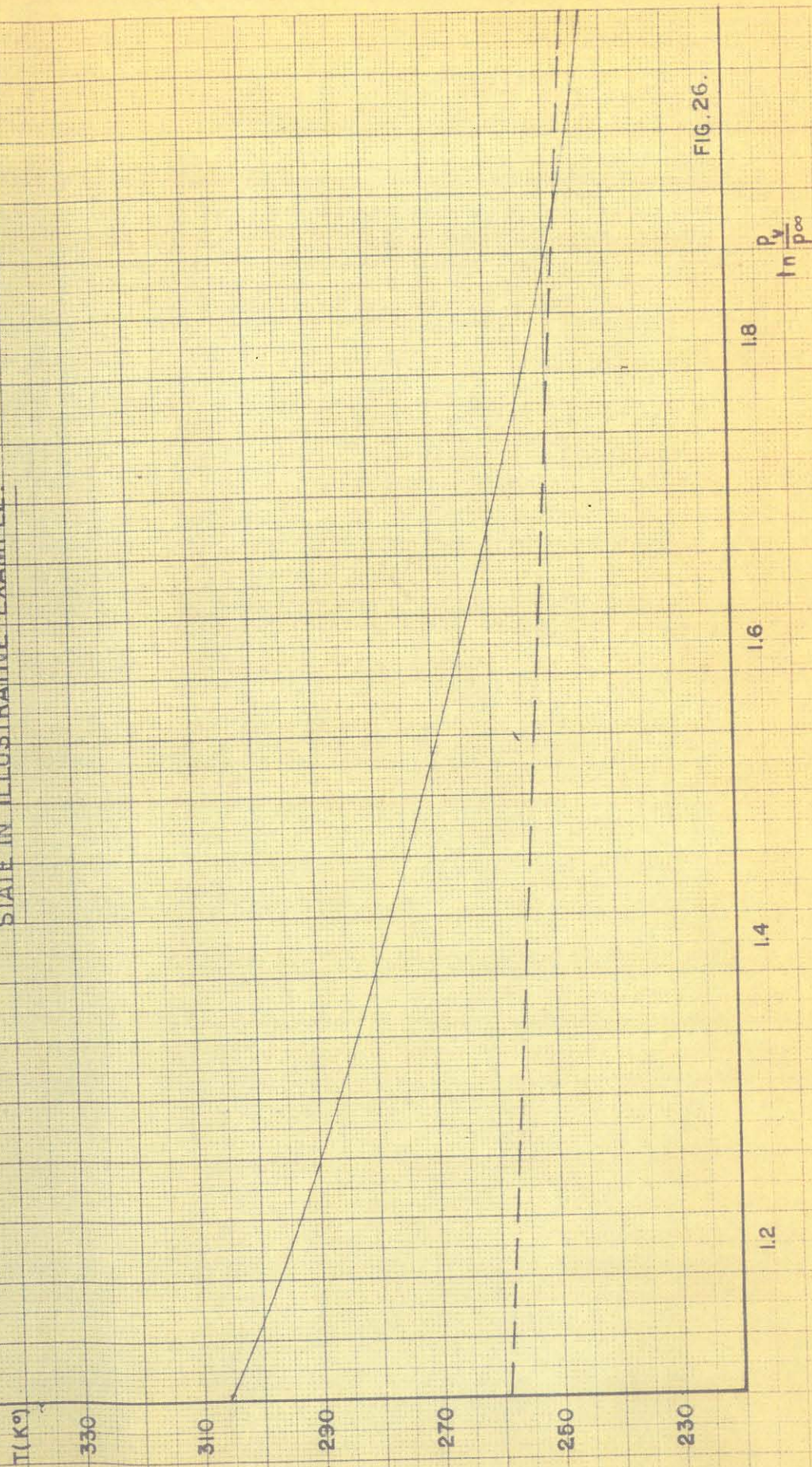


FIG. 26.



RELATIONSHIP BETWEEN SUPERSATURATION PRESSURE RATIO AND  $\alpha_x$

$$\alpha_x = \frac{2x}{d_t}$$

where X = DISTANCE DOWNSTREAM FROM THROAT  
 $d_t$  = THROAT DIAMETER

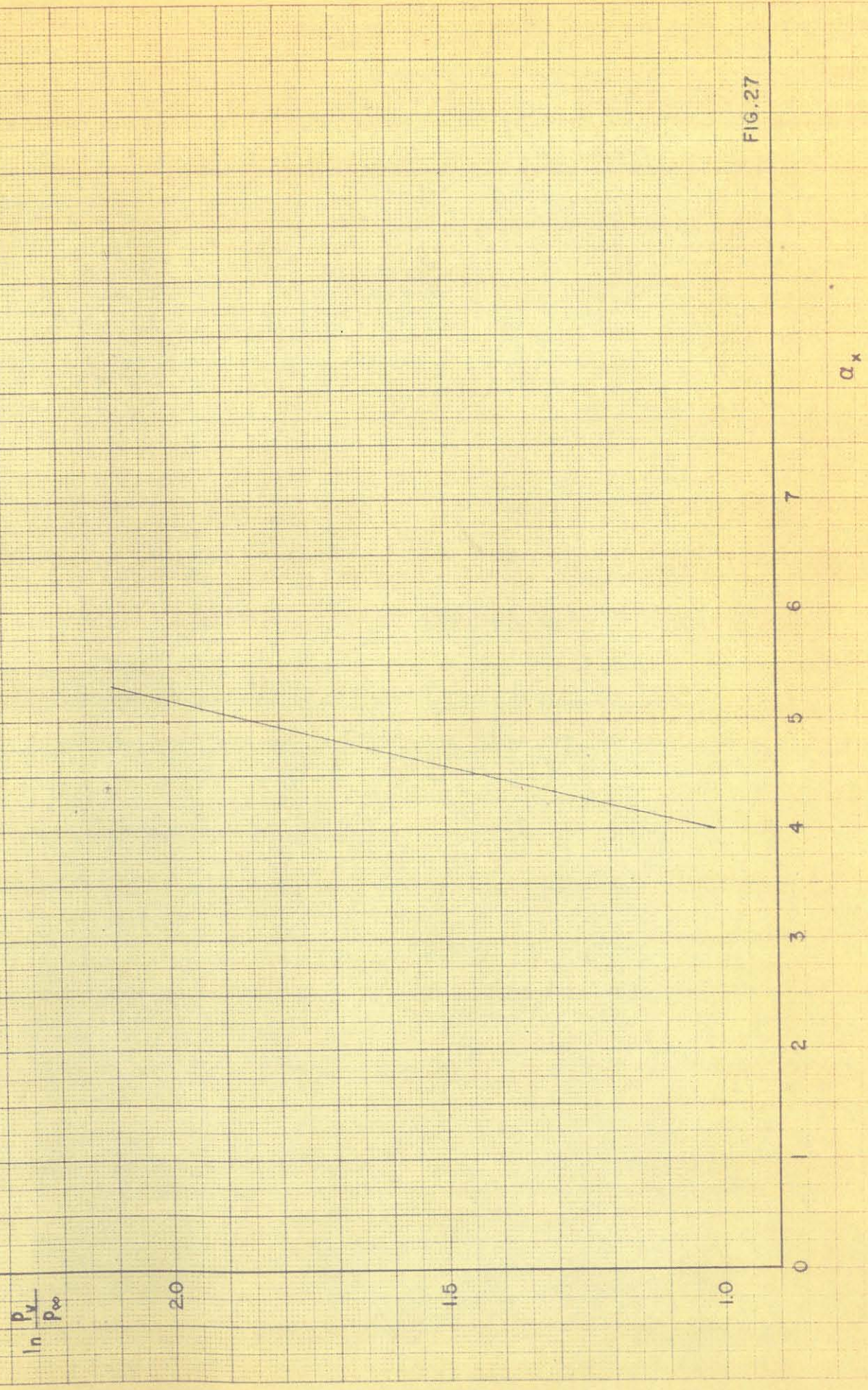


FIG. 27



NOTATION IN TREATMENT OF  
OBLIQUE CONDENSATION SHOCK

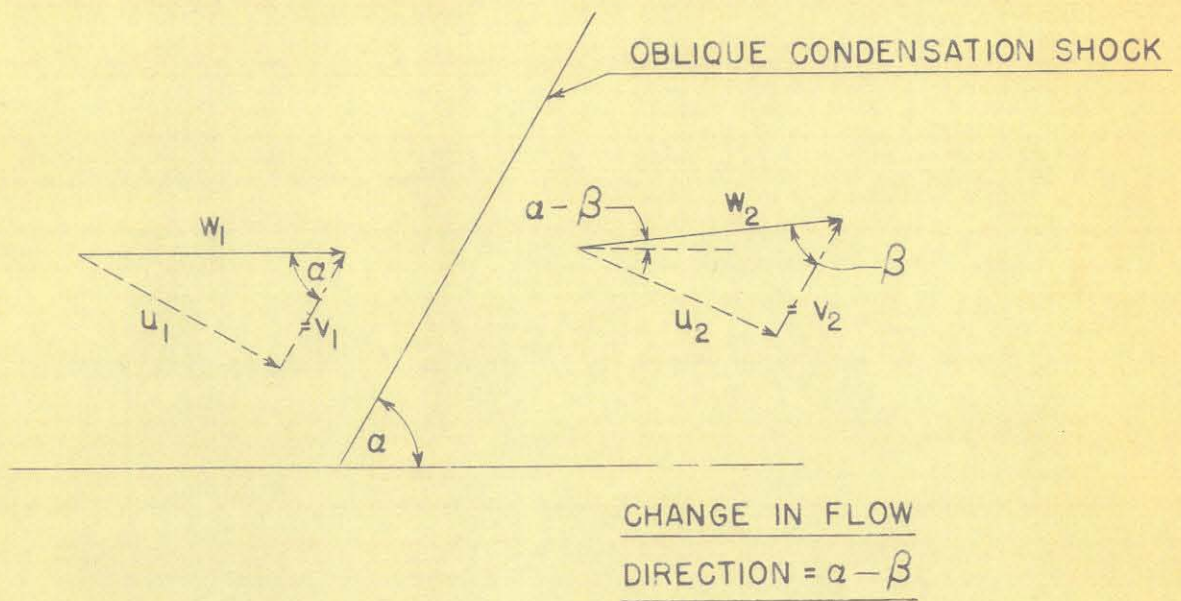


FIG. 28



CHANGE IN DIRECTION OF FLOW THROUGH  
OBLIQUE CONDENSATION SHOCK.



$M_1 = 1.3$

$\frac{M_2}{M_1} = .8$

$\frac{M_2}{M_1} = .85$

$\frac{M_2}{M_1} = .9$

$\frac{M_2}{M_1} = .95$

$\frac{M_2}{M_1} = 1$

$\alpha - \beta$

6°

5°

4°

3°

2°

1°

0°

25°

50°

75°

100°

$\alpha$

FIG. 29



CHANGE IN DIRECTION OF FLOW THROUGH  
OBLIQUE CONDENSATION SHOCK.



$M_1 = 2.0$

$\alpha - \beta$

$\frac{M_2}{M_1} = 5$

$\frac{M_2}{M_1} = 5.5$

$\frac{M_2}{M_1} = 6$

$\frac{M_2}{M_1} = 6.5$

$\frac{M_2}{M_1} = 7$

$\frac{M_2}{M_1} = 8$

$\frac{M_2}{M_1} = 9$

$\alpha$

25°

50°

75°

100°

FIG. 30



CHANGE IN DIRECTION OF FLOW THROUGH  
OBLIQUE CONDENSATION SHOCK.



$M_1 = 2.5$

$\frac{M_2}{M_1} = .4$

$\frac{M_2}{M_1} = .45$

$\frac{M_2}{M_1} = .5$

$\frac{M_2}{M_1} = .55$

$\frac{M_2}{M_1} = .6$

$\frac{M_2}{M_1} = .7$

$\frac{M_2}{M_1} = .8$

$\frac{M_2}{M_1} = .9$

$\alpha - \beta$

12°

11°

10°

9°

8°

7°

6°

5°

4°

3°

2°

1°

0°

25°

50°

75°

100°

$\alpha$

FIG. 31



CHANGE IN DIRECTION OF FLOW THROUGH  
OBLIQUE CONDENSATION SHOCK



$M_1 = 3.0$

$\alpha - \beta$

17°  
16°  
15°  
14°  
13°  
12°  
11°  
10°  
9°  
8°  
7°  
6°  
5°  
4°  
3°  
2°  
1°  
0°

$\frac{M_2}{M_1} = .35$

$\frac{M_2}{M_1} = .4$

$\frac{M_2}{M_1} = .45$

$\frac{M_2}{M_1} = .5$

$\frac{M_2}{M_1} = .6$

$\frac{M_2}{M_1} = .7$

$\frac{M_2}{M_1} = .8$

$\frac{M_2}{M_1} = .9$

100°

$\alpha$

75°

50°

25°

0°

FIG.32



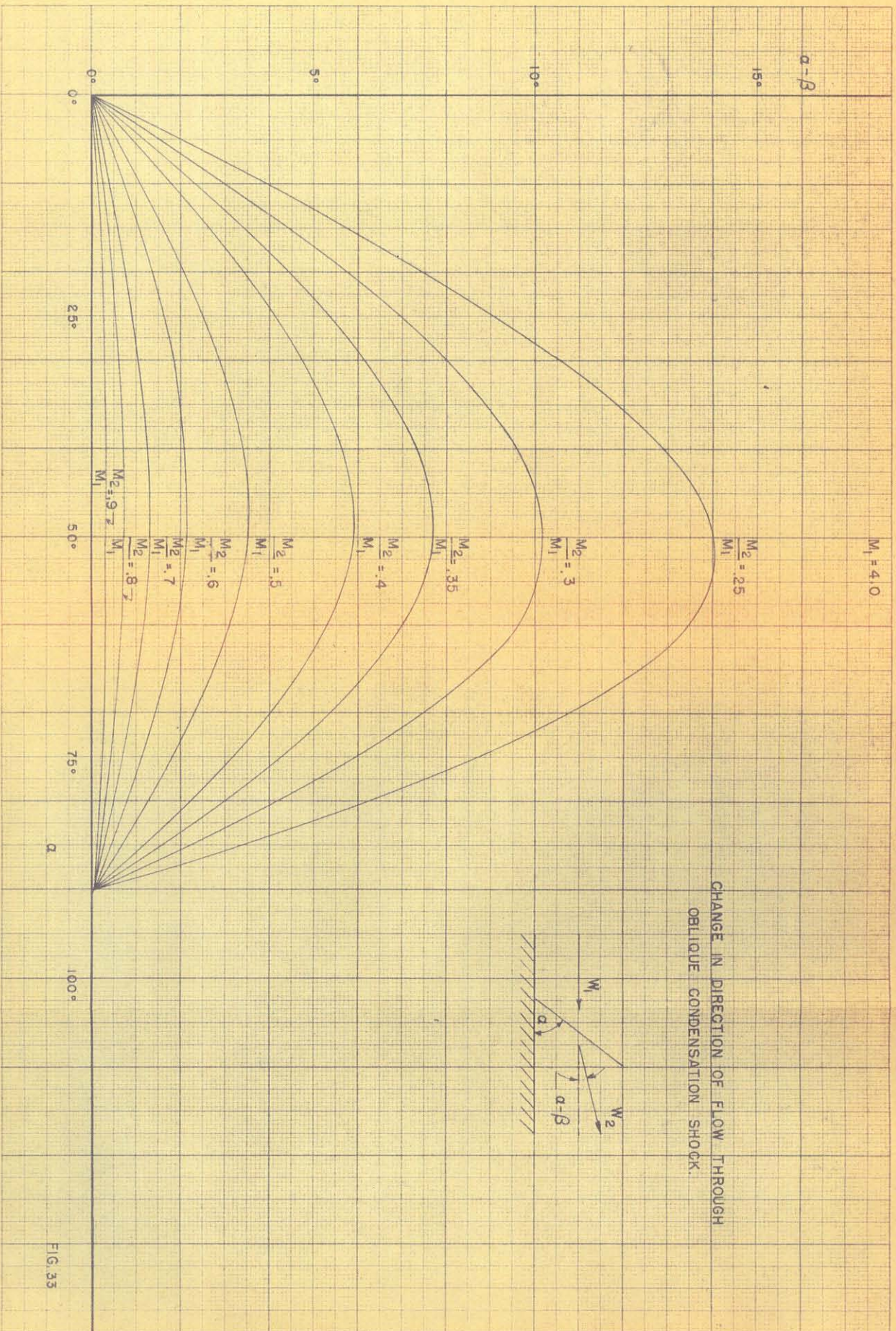


FIG. 33